NASA MEMO 2-9-59L

NASA MEMORANDUM

AN EXPERIMENTAL STUDY AT A MACH NUMBER OF 3 OF THE EFFECT OF TURBULENCE LEVEL AND SANDPAPER-TYPE ROUGHNESS ON TRANSITION ON A FLAT PLATE

By Robert A. Jones

Langley Research Center
Langley Field, Va.

NATIONAL AERONAUTICS AND SPACE ADMINISTRATION
WASHINGTON
March 1959

NATIONAL AERONAUTICS AND SPACE ADMINISTRATION

MEMORANDUM 2-9-59L

AN EXPERIMENTAL STUDY AT A MACH NUMBER OF 3 OF THE EFFECT OF TURBULENCE LEVEL AND SANDPAPER-TYPE ROUGHNESS ON TRANSITION ON A FLAT PLATE

By Robert A. Jones

SUMMARY

An investigation has been conducted at a Mach number of 3 of the effect of turbulence level and sandpaper-type roughness on transition for a flat plate. The Reynolds number varied from 0.8×10^6 to 1.8×10^6 per inch; the settling-chamber turbulence level varied from 0.7 percent to 35 percent; and the heat transfer between the plate and the stream was negligible. Transition locations were determined by an optical method. This method was indicative of a permanent change in the boundary-layer density distribution rather than the onset of turbulent bursts. Results showed that, when transition was influenced by roughness, it moved in a way similar to its movement on a smooth plate. That is, it gradually approached the roughness location with either an increase in unit Reynolds number or an increase in turbulence level.

For roughness submerged in the linear portion of the boundary-layer velocity profile, the square root of the roughness Reynolds number and the ratio of roughness height to boundary-layer displacement thickness gave similar results as parameters for predicting the effects of roughness. A range of each of these parameters which moved transition less than 10 percent was found and this range was a function of turbulence level.

INTRODUCTION

The effect of roughness on the flow in a boundary layer has been considered in two essentially different ways. One way is to consider the roughness as having an effect when turbulent spots begin to appear downstream of the roughness. The point where these turbulent spots begin to appear can be detected by a hot wire located in the boundary layer. The other way is to consider roughness as having an effect when these turbulent spots become significant enough to make a permanent ar pronounced change in the boundary-layer velocity and density distribu .on.

The point where this change in velocity and density distribution begins to take place can be detected by total-pressure surveys, schlieren and shadowgraph pictures, heat-transfer measurements, sublimation of solids, phosphorescent films, and so forth.

A direct comparison of data obtained by these two methods can not be made since, when the turbulent spots first appear, they may not be frequent enough or may not be of a large enough size to make a permanent change in the boundary-layer velocity and density profiles.

A review of low-speed data on the effect of two-dimensional roughness on transition as indicated by permanent changes in the boundary-layer velocity and density profiles given in reference 1 indicated that the ratio of roughness height k to the displacement thickness at the roughness location δ_k^* is a better representation of the data than a constant critical Reynolds number R_k of the roughness element. The data of reference 2 were correlated according to the former parameter and indicated that for two-dimensional roughness three to seven times the value of k/δ_k^* at low speeds was necessary to effect transition at a Mach number of 3.

In reference 3, a comparison was made between the effect of two- and three-dimensional roughness on transition as indicated by the onset of turbulent bursts (first method) at low speeds. For two-dimensional roughness, there was a relationship between transition Reynolds number R_t and k/δ_k^* similar to that found in reference 1. Three-dimensional results failed to satisfy such a relation. With three-dimensional roughness there was no effect until a value of R_k was reached which brought transition to the roughness location.

A low-speed investigation of the effect of distributed granular-type roughness on transition reported in reference 4 indicated that, when the roughness is submerged in the linear portion of the local boundary-layer velocity profile, turbulent spots begin to appear immediately behind the roughness when a critical R_k of approximately 600 was reached. This investigation was extended in reference 5 to Mach numbers of 1.6 and 2.0 and indicated that turbulent spots begin to appear at supersonic speeds at approximately the same critical R_k.

Several previous investigations have studied the effects of tunnel-turbulence level on transition for smooth models. (See refs. 6 to 9.) Transition location as indicated by a permanent change in the velocity and density distribution was found to be a function of turbulence level; however, no consistent trends were found. No studies are known which include the effects of turbulence level on transition influenced by roughness.

The present investigation was conducted to study the effect of settling-chamber turbulence level on transition as indicated by a permanent change in the velocity and density distributions on a flat plate with and without roughness at a Mach number of 3 and with zero heat transfer. Results will be presented in terms of the parameters R_k and k/δ_k^* for three sizes of distributed roughness in strips at various locations and pressure levels and for three settling-chamber turbulence levels.

SYMBOLS

ρ	local density
k	height of roughness element, in.
M	Mach number
x	distance from leading edge, in.
u	local streamwise component of velocity
ν	local coefficient of kinematic viscosity
R	Reynolds number
R_k	roughness Reynolds number, $\frac{u_k k}{\nu_k}$
δ^*	boundary-layer displacement thickness, $\int_0^\infty \left(1 - \frac{\rho u}{\rho_\infty u_\infty}\right) dy$
u'	root-mean-square longitudinal turbulent velocity component in settling chamber
y	distance normal to the surface

Subscripts:

k	conditions at top of roughness element
t	conditions at beginning of transition
t'	conditions at end of transition

o conditions for smooth plate

∞ conditions for free stream

APPARATUS

Wind Tunnel

All tests were conducted in a Mach number 3 blowdown tunnel of the Langley gas dynamics laboratory. The nozzle of this tunnel was two-dimensional. The top of the nozzle was made of steel lined with plastic and was contoured for $M = 3$ flow. The bottom of the nozzle was a flat steel plate. (See fig. 1.) The test section measured 5 by 8 inches in cross section and had a Mach number distribution of 3.05 ± 0.04. A range of settling-chamber pressures of 55 to 125 pounds per square inch gage and a constant settling-chamber temperature of 100° F were used for these tests. These conditions resulted in a Reynolds number range from 0.8×10^6 to 1.8×10^6 per inch.

The settling chamber of this tunnel was long and readily accessible; thus it was possible to operate the tunnel at different turbulence levels by changing the settling-chamber configuration. The configuration causing the highest turbulence level consisted of a perforated cone supported by a ring at its base. This cone was used to break up the large eddies in the flow and not to generate turbulence. A lower turbulence level was obtained when this cone was followed by four fine-mesh-wire damping screens. The lowest turbulence level was obtained by using two porous plates having a total pressure drop ranging from 30 to 70 pounds per square inch as damping screens. These plates were located downstream of the perforated cone. (See fig. 1.)

Model

The model was a flat plate 12 inches long, made of steel, and spanned the test section. It had a leading-edge wedge angle of 14°. The leading edge was rounded and its thickness was kept between 0.006 and 0.007 inch. The finish of the plate was approximately 200 micro-inches. The variation of Mach number as determined by static-pressure probes along the forward portion of the plate is shown in figure 2. The plate was supported by a 1/8-inch-thick steel channel fastened to the underside of the plate and to the test-section side walls.

TEST METHODS AND TECHNIQUES

Hot-Wire Determination of Turbulence Level

Measurements of the longitudinal turbulence intensity were made at several radial locations in a plane 5 inches downstream from the last screen in the settling chamber. The mean-flow velocity was approximately 30 feet per second in this plane. A hot-wire probe employing tungsten wire 0.0003 inch in diameter and 0.125 inch long was used. The longitudinal turbulence intensity was taken as the average of several measurements and, within their accuracy ($\pm$0.2 percent at the low-turbulence level), was determined to be a constant over the range of test pressures for each settling-chamber configuration.

The actual values of turbulence intensity are only qualitative. The settling-chamber turbulence level was recorded since the test-section-turbulence level could not be measured because of wire failures. The effect of tunnel contraction on the intensity of turbulence in the test section is dependent on the character of the settling-chamber turbulence; however, the test-section turbulence may have been considerably less than the measured intensity in the settling chamber.

Transition Determination by Shadowgraphs

The location of transition was determined optically by a method used in references 10 and 11. In this method, photographic film was placed on a parallel-motion mechanism which enabled the distance from the model to the film to be adjusted in order to take advantage of focusing effects caused by the refraction of light as it passes through the boundary layer. The white laminar line appeared to be displaced from the surface by a distance that is large compared with the boundary-layer thickness. The displacement was nearly constant as long as the layer remained laminar since the density profiles were nearly similar along the plate length. The beginning of a change in the slope of this laminar line represented the beginning of transition effects on the density profile and was taken as the beginning of transition itself. Thus, this is a method which indicates a permanent change in the density profile and is different from the method used in references 3 to 5. The end of convergence represented the end of transition. An example is illustrated for the smooth plate in figure 3. The arrows indicate the beginning of transition; this point was taken as the transition location. At least two shadowgraphs were made for each test point. The transition point measured by the shadowgraphs agreed within 0.2 inch for each test point. The exposure time of the flash was between 5 and 6 microseconds.

Transition Determination by Sublimating Solid

Transition was also determined by the sublimation of acenaphthene crystals sprayed on the plate. (See ref. 12.) The procedure was to spray the plate with a saturated solution of acenaphthene, allow the solution to dry, and then mount the plate in the test section. The tunnel was run until the transition pattern became clear, then it was shut down, and the plate removed and photographed.

In order to determine whether the crystals themselves affected transition, transition was determined by the shadowgraph technique for the smooth plate and for the smooth plate sprayed with acenaphthene crystals. No effect of the crystals on transition was noticed.

Photographs of the plate showing the pattern of transition downstream of a roughness strip are presented in figure 4. In these photographs a strip of 0.002-inch roughness elements 1/8 inch wide was located 1/2 inch from the leading edge. The acenaphthene crystals covered the entire portion of the plate from 1/8 inch downstream of the roughness to the end of the plate.

Determination of Roughness Size

Roughness of three sizes and composed of aluminum-oxide particles was used. The strip to be coated with roughness was sprayed with a very thin coating of lacquer, and then the roughness particles were sprayed on by means of an artist's air brush. Applying the roughness in this manner produced a uniform distribution of roughness which adhered well to the plate. Photographs of sample roughness strips are presented in figure 5. The maximum height of the roughness particles was determined by laying a parallel bar over the roughness strip and measuring its displacement from the plate at several spanwise locations before and after testing. Small areas of roughness 1/4 inch by 1/8 inch were checked and were found to have the same maximum displacement. The maximum displacement was found to be constant for different roughness strips of the same particle size and was taken to be the roughness height.

RESULTS AND DISCUSSION

Tabular Presentation of Results

All the principal results and parameters are given in table I in order to permit possible comparison in other forms and with parameters other than those discussed herein if desired. For these results,

transition locations were obtained from shadowgraphs. The width of the roughness strip in every case was 1/8 inch and the distance from the leading edge to the roughness location x_k was measured to the center of the strip. Values of $\sqrt{R_k}$ and δ_k^* were calculated from velocity and temperature distributions through the boundary layer obtained by the methods of reference 13 and from the viscosity obtained by Sutherland's law. The static pressure was assumed to be constant across the boundary layer. For these calculations, the maximum value of k as described under "Determination of Roughness Size" was used.

Certain peculiarities in the data should be noted. The data for which transition occurred at the roughness location are indicated in the column headed "Transition at x_k." In every case, the distance to transition x_t is larger than the distance to the roughness location x_k. This difference is due in part to the peculiarities of the method of indicating transition. It was noticed during the experiments that transition, as indicated by shadowgraphs, gradually approached x_k as the unit Reynolds number $\frac{u_\infty}{\nu_\infty}$ increased until it reached a certain small distance from x_k. Upon reaching this location, an increase in $\frac{u_\infty}{\nu_\infty}$ would not continue to move transition and it was assumed that transition was fixed at the roughness. It is believed that, when transition is at the roughness, the disturbance waves from the roughness may affect the slope of the laminar white line. (See fig. 6.) In figure 6 a strip of 0.002-inch roughness is located 1.5 inches from the leading edge.

It should also be noted that there are several points for which transition caused by roughness is farther downstream than transition of the smooth plate $(x_t > x_{t,o})$. A large part of this difference is due to the scatter in the data; however, because of the peculiarity of the method of indicating transition, as the roughness location nears the location of transition for the smooth plate these points would appear downstream of the natural transition point.

Results for the Smooth Plate

The effect of settling-chamber turbulence level on transition Reynolds number for the smooth plate is shown in figure 7. A maximum transition Reynolds number of 3.7×10^6 was obtained at a unit Reynolds number of 1.77×10^6 per inch and a settling-chamber turbulence level of 0.7 percent. In general, at a given unit Reynolds number, when the turbulence level was decreased, the transition Reynolds number increased.

At the low turbulence level, the transition Reynolds number increased steadily with an increase in unit Reynolds number while at the two higher turbulence levels the transition Reynolds number increased initially but at higher unit Reynolds numbers it decreased. No explanation for this reversal at the higher turbulence level was found.

Results for Sandpaper-Type Roughness

The transition pattern behind roughness as obtained with the sublimation technique is shown in figure 4. The mean location of transition varied across the span of the plate. (See figs. 4(a) and 4(b).) This is believed to be due to the interaction of the nozzle wall boundary layer with the plate boundary layer. Superimposed on this spanwise variation was a streamwise variation of transition location.

The shadowgraph indicates the point across the span where the transition effects first make a change in the boundary-layer density profile and the point where the boundary layer becomes completely turbulent across the span. The beginning and end of transition as indicated by the shadowgraphs agreed fairly well with the beginning and end of the transition region indicated by the sublimation technique in the center portion of the plate. Therefore, it is assumed that the transition point indicated by the shadowgraph technique is one which takes into account the random streamwise fluctuations and is not significantly affected by mean variation along the span caused by the interaction of the plate and nozzle wall boundary layers.

A few tests were made to determine the effect of the width of the roughness strip on transition. Tests were made for two roughness heights for the entire plate downstream of 15/16 inch covered with roughness. These results are compared with those for a 1/8-inch strip located the same distance from the leading edge of the plate in figure 8. The wide strip moved transition further forward on the plate than did the 1/8-inch strip. This effect may be due to the wider strip having a larger number of maximum size particles. With the exception of figure 8, all the data in this report are for a 1/8-inch-wide roughness strip.

Transition locations obtained from shadowgraphs are given as a function of roughness location x_k for the turbulence levels $\frac{u'}{u}$ in figures 9 to 12 for roughness heights k of 0.002, 0.003, and 0.005 inch. The solid symbols indicate transition essentially at the roughness location. Also included are the transition locations for the smooth plate ($k = 0$) indicated by the dashed lines. Note that for the 0.005-inch roughness height, transition was always located at the roughness location.

Certain general trends may be deduced from these figures. When transition was influenced by roughness, it moved in a way similar to its movement on the smooth plate, that is, it gradually moved forward with either an increase in $\frac{u_\infty}{\nu_\infty}$ or an increase in $\frac{u'}{u}$ until it reached the roughness location. The gradual decrease in x_t with an increase in $\frac{u_\infty}{\nu_\infty}$ was a trend similar to that for two-dimensional roughness at low speeds reported in references 1 and 3 but is different from the results of distributed roughness at low speeds reported in references 3 and 4 where it was found that roughness either had no effect on transition or moved transition to the roughness element. It is believed that this difference is due to the difference in the transition criteria as discussed in the "Introduction" and that a direct comparison is not valid.

Another trend to be noted is that an increase in turbulence caused transition to move forward except where transition was located at the roughness.

Values of $\sqrt{R_k}$ are shown plotted against R_t for each turbulence level in figure 13. The square root of the roughness Reynolds number was used as it is more near linearly proportional to the projection height for roughness submerged in the linear portion of the boundary-layer velocity profile. Values of k/δ_k^* are shown plotted against R_t for each turbulence level in figure 14. In figures 13 and 14 the data for which transition is fixed at the roughness strip (solid symbols) or for which transition is not affected by the presence of the roughness strip (flagged symbols) are valid only as indications of the boundaries of the functional relationships which are plotted. A large similarity between $\sqrt{R_k}$ and k/δ_k^* as parameters for predicting the effect of roughness on transition is evident. With both parameters and the two smaller values of k the minimum values required to fix transition essentially at the roughness varied with k for a given $\frac{u'}{u}$ and varied with $\frac{u'}{u}$ for a given k.

Values of $\sqrt{R_k}$ and $\frac{k}{\delta_k^*}$ are shown plotted against $\frac{R_t}{R_{t,o}}$ in figures 15 and 16 for all turbulence levels. Here again, the similarity between the two parameters is evident. It is also evident that plotting of these parameters as functions of $\frac{R_t}{R_{t,o}}$ does not take into account the effect of turbulence on transition. This may be due to turbulence having a larger effect on transition for larger roughness.

The range of $\sqrt{R_k}$ and $\frac{k}{\delta_k^*}$ which moved transition less than 10 percent $\left(0.9x_{t,o} \leqq x_t \leqq x_{t,o}\right)$ is shown as a function of turbulence level in figures 17 and 18. The range of 12 to 25 in $\sqrt{R_k}$ at the low turbulence level is approximately the same as the range of critical roughness Reynolds number reported in reference 4 at low speeds and reported in reference 5 at $M = 1.6$ and 2.0. It must be noted that the transition criteria are different in these cases and thus a direct comparison is not valid.

A comparison of the present data in terms of $\frac{k}{\delta_k^*}$ as a function of $\frac{R_t}{R_{t,o}}$ with the low-speed two-dimensional data of reference 1 and with the $M = 3$ two-dimensional data of reference 2 is presented in figure 19. It can be seen that three-dimensional distributed roughness has a greater influence on transition than does two-dimensional roughness at a Mach number of 3.

CONCLUSIONS

An optical method was used to study the effect of settling-chamber turbulence level and sandpaper-type roughness on transition for a flat plate at a Mach number of 3. This method was indicative of a permanent change in the boundary-layer-density distribution rather than the onset of turbulent bursts and indicated the following:

1. When transition is influenced by roughness, it moves in a way similar to its movement on a smooth plate. That is, it gradually approaches the roughness location with either an increase in unit Reynolds number or an increase in turbulence level.

2. When the roughness is submerged in the linear portion of the boundary-layer velocity profile, the square root of the roughness Reynolds number and the ratio of roughness height to boundary-layer displacement thickness give similar results when used as parameters for predicting the effect of roughness.

3. A range of either of these parameters which will move transition less than 10 percent can be found and is a function of turbulence level. When the turbulence level is high, this range is approximately constant; as the level of turbulence is lowered, the upper limit of this range may increase.

Langley Research Center,
National Aeronautics and Space Administration,
Langley Field, Va., October 30, 1958.

REFERENCES

1. Dryden, Hugh L.: Review of Published Data on the Effect of Roughness on Transition From Laminar to Turbulent Flow. Jour. Aero. Sci., vol. 20, no. 7, July 1953, pp. 477-482.

2. Brinich, Paul F.: Boundary-Layer Transition at Mach 3.12 With and Without Single Roughness Elements. NACA TN 3267, 1954.

3. Klebanoff, P. S., Schubauer, G. B., and Tidstrom, K. D.: Measurements of the Effect of Two-Dimensional and Three-Dimensional Roughness Elements on Boundary-Layer Transition. Jour. Aero. Sci., vol. 22, no. 11, Nov. 1955, pp. 803-804.

4. Von Doenhoff, Albert E., and Horton, Elmer A.: A Low-Speed Experimental Investigation of the Effect of a Sandpaper Type of Roughness on Boundary-Layer Transition. NACA Rep. 1349, 1958. (Supersedes NACA TN 3858.)

5. Braslow, Albert L.: Effect of Distributed Granular-Type Roughness on Boundary-Layer Transition at Supersonic Speeds With and Without Surface Cooling. NACA RM L58A17, 1958.

6. Evvard, J. C., Tucker, M., and Burgess, W. C., Jr.: Statistical Study of Transition-Point Fluctuations in Supersonic Flow. NACA TN 3100, 1954.

7. Laufer, John, and Marte, Jack E.: Results and a Critical Discussion of Transition-Reynolds-Number Measurements on Insulated Cones and Flat Plates in Supersonic Wind Tunnels. Rep. No. 20-96 (Contract No. DA-04-495-Ord 18), Jet Propulsion Lab., C.I.T., Nov. 30, 1955.

8. Ross, Albert O.: Determination of Boundary-Layer Transition Reynolds Numbers by Surface-Temperature Measurement of a 10° Cone in Various NACA Supersonic Wind Tunnels. NACA TN 3020, 1953.

9. Lange, A. H., and Gieseler, L. P.: Measurement of Boundary-Layer Transition on a Standard Model To Determine the Relative Disturbance Level in Two Supersonic Wind Tunnels. NAVORD Rep. 2752 (Aeroballistic Res. Rep. 170), U. S. Naval Ord. Lab. (White Oak, Md.), Feb. 19, 1953.

10. Pearcey, H. H. The Indication of Boundary-Layer Transition on Aerofoils in the N.P.L. 20 In. × 8-In. High Speed Wind Tunnel. CP No. 10 (11, 991), British A.R.C., Dec. 14, 1948.

11. Chapman, Dean R., Kuehn, Donald M., and Larson, Howard K.: Investigation of Separated Flows in Supersonic and Subsonic Streams With Emphasis on the Effect of Transition. NACA TN 3869, 1957.

12. Main-Smith, J. D.: Chemical Solids as Diffusible Coating Films for Visual Indications of Boundary-Layer Transition in Air and Water. R. & M. No. 2755, British A.R.C., 1950.

13. Low, George M.: The Compressible Laminar Boundary Layer With Fluid Injection. NACA TN 3404, 1955.

TABLE I.- PRESENTATION OF RESULTS

(a) $\frac{u'}{u}$ = 0.7 percent

k, in.	x_k, in.	$\frac{u_\infty}{\nu_\infty}$, per inch	$\sqrt{R_k}$	δ_k^*, in.	$\frac{k}{\delta_k^*}$	Transition at x_k	x_t, in.	R_t	$\frac{R_t}{R_{t,o}}$	x_t', in.
0	----	0.885×10^6	-----	-------	-----	No	3.7	3.28×10^6	-----	4.4
0	----	1.33	-----	-------	-----	No	2.6	3.46	-----	3.2
0	----	1.77	-----	-------	-----	No	2.1	3.74	-----	2.8
.002	0.25	.885	14.73	0.00288	0.695	No	3.0	2.66	0.810	3.9
.002	.25	1.33	21.70	.00235	.850	No	1.7	2.26	.765	2.1
.002	.25	1.77	29.55	.00204	.980	No	1.0	1.77	.475	1.3
.002	.50	.885	11.49	.00408	.490	No	3.4	3.01	.915	4.0
.002	.50	1.33	16.16	.00328	.610	No	2.3	3.06	.880	2.6
.002	.50	1.77	20.86	.00238	.840	No	1.3	2.30	.618	1.7
.002	.75	.885	10.10	.00500	.400	No	3.4	3.01	.915	3.9
.002	.75	1.33	14.07	.00408	.490	No	1.9	2.53	.728	2.4
.002	.75	1.77	17.86	.00353	.566	No	1.35	2.39	.642	1.7
.002	1.00	.885	9.27	.00577	.347	No	3.3	2.92	.890	4.0
.002	1.00	1.33	12.73	.00471	.424	No	2.5	3.32	.955	3.0
.002	1.00	1.77	16.28	.00408	.490	No	1.6	2.83	.760	2.0
.002	1.25	.885	8.77	.00645	.310	No	3.6	3.18	.967	4.0
.002	1.25	1.33	12.04	.00526	.380	No	2.7	3.59	1.04	3.3
.002	1.25	1.77	15.10	.00456	.438	No	2.0	3.54	.950	2.4
.002	1.50	.885	8.37	.00707	.283	No	3.6	3.18	.967	4.3
.002	1.50	1.33	11.40	.00576	.347	No	2.8	3.72	1.07	3.3
.002	1.50	1.77	14.25	.00500	.400	No	2.4	4.25	1.14	2.7
.002	1.75	.885	8.00	.00763	.262	No	3.5	3.10	.945	4.3
.002	1.75	1.33	10.95	.00623	.321	No	2.6	3.46	1.00	3.3
.002	1.75	1.77	13.64	.00540	.370	No	2.3	4.07	1.09	2.6

TABLE I.- PRESENTATION OF RESULTS - Continued

(a) $\frac{u'}{u}$ = 0.7 percent - Continued

k, in.	x_k, in.	$\frac{u_\infty}{\nu_\infty}$, per inch	$\sqrt{R_k}$	δ_k^*, in.	$\frac{k}{\delta_k^*}$	Transition at x_k	x_t, in.	R_t	$\frac{R_t}{R_{t,o}}$	x_t', in.
0.003	0.25	0.885×10^6	28.02	0.00288	1.04	No	1.3	1.15×10^6	0.351	2.0
.003	.25	1.33	45.25	.00235	1.28	Yes	.8	1.07	.308	1.1
.003	.25	1.77	63.84	.00204	1.47	Yes	.8	1.42	.381	.9
.003	.50	.885	18.36	.00408	.735	No	2.9	2.57	.784	3.5
.003	.50	1.33	28.41	.00328	.915	No	1.6	2.13	.615	2.1
.003	.50	1.77	38.94	.00238	1.26	Yes	.8	1.42	.381	1.1
.003	.75	.885	16.31	.00500	.600	No	3.7	3.28	1.00	4.2
.003	.75	1.33	23.19	.00408	.735	No	2.1	2.80	.810	2.3
.003	.75	1.77	30.66	.00353	.849	No	1.3	2.30	.618	1.7
.003	1.0	.885	14.66	.00577	.520	No	3.8	3.54	1.08	4.5
.003	1.0	1.33	20.71	.00471	.637	No	2.5	3.59	1.04	3.1
.003	1.0	1.77	26.83	.00408	.735	No	1.6	3.18	.855	2.2
.003	1.25	.885	13.60	.00645	.465	No	3.7	3.28	1.00	4.5
.003	1.25	1.33	19.10	.00526	.570	No	2.6	3.06	.885	3.1
.003	1.25	1.77	24.41	.00456	.658	No	1.6	2.83	.760	2.3
.003	1.50	.885	12.81	.00707	.424	No	3.7	3.28	1.00	4.5
.003	1.50	1.33	17.97	.00576	.520	No	2.5	3.32	.960	3.0
.003	1.50	1.77	22.85	.00500	.600	No	1.9	3.36	.903	2.4
.003	1.75	.885	12.29	.00763	.394	No	3.7	3.28	1.00	4.4
.003	1.75	1.33	17.06	.00623	.481	No	2.5	3.32	.960	3.0
.003	1.75	1.77	21.59	.00540	.556	No	2.1	3.72	1.00	2.6
.003	2.00	.885	11.83	.00815	.368	No	3.7	3.28	1.00	4.3
.003	2.00	1.33	16.37	.00666	.450	No	2.5	3.32	.960	2.9

TABLE I.- PRESENTATION OF RESULTS - Continued

(a) $\frac{u'}{u}$ = 0.7 percent - Concluded

k, in.	x_k, in.	$\frac{u_\infty}{\nu_\infty}$, per inch	$\sqrt{R_k}$	δ_k^*, in.	$\frac{k}{\delta k^*}$	Transition at x_k	x_t, in.	R_t	$\frac{R_t}{R_{t,o}}$	x_t', in.
0.005	0.50	0.885×10^6	44.94	0.00288	1.74	Yes	0.6	0.53×10^6	0.162	1.2
.005	.50	1.33	73.21	.00235	2.13	Yes	.6	.80	.231	.9
.005	.50	1.77	92.74	.00204	2.45	Yes	.6	1.06	.286	.9
.005	.75	.885	33.84	.00408	1.22	Yes	.9	.80	.243	1.4
.005	.75	1.33	55.07	.00328	1.52	Yes	.9	1.20	.346	1.1
.005	.75	1.77	78.19	.00238	2.10	Yes	.9	1.60	.428	1.1
.005	1.0	.885	28.62	.00500	1.00	Yes	1.2	1.06	.325	1.8
.005	1.0	1.33	44.74	.00408	1.22	Yes	1.2	1.60	.461	1.4
.005	1.0	1.77	63.58	.00353	1.41	Yes	1.2	2.12	.572	1.4
.005	1.25	.885	25.61	.00577	.867	Yes	1.4	1.24	.379	2.2
.005	1.25	1.33	38.92	.00471	1.06	Yes	1.4	1.86	.539	2.0
.005	1.25	1.77	53.94	.00408	1.22	Yes	1.4	2.48	.666	2.0
.005	1.50	.885	24.27	.00645	.775	Yes	1.7	1.57	.460	2.7
.005	1.50	1.33	35.10	.00526	.950	Yes	1.7	2.36	.654	2.1
.005	1.50	1.77	47.92	.00456	1.10	Yes	1.7	3.13	.809	2.0
.005	1.75	.885	22.27	.00707	.708	Yes	1.9	1.68	.514	2.8
.005	1.75	1.33	32.45	.00576	.868	Yes	1.9	2.53	.731	2.4
.005	1.75	1.77	44.26	.00500	1.00	Yes	1.9	3.36	.905	2.2
.005	2.00	.885	20.93	.00763	.655	Yes	2.2	1.94	.595	3.0
.005	2.00	1.33	30.56	.00623	.803	Yes	2.1	2.80	.809	2.7
.005	2.00	1.77	40.45	.00540	.925	Yes	2.1	3.72	1.00	2.4

TABLE I.- PRESENTATION OF RESULTS - Continued

(b) $\frac{u'}{u}$ = 1.5 percent

k, in.	x_k, in.	$\frac{u_\infty}{\nu_\infty}$, per inch	$\sqrt{R_k}$	δ_k^*, in.	$\frac{k}{\delta_k^*}$	Transition at x_k	x_t, in.	R_t	$\frac{R_t}{R_{t,o}}$	x_t', in.
0	---	0.885×10^6	-----	-------	-----	---	3.3	2.92×10^6	-----	4.3
0	---	1.33	-----	-------	-----	---	2.5	3.32	-----	3.2
0	---	1.77	-----	-------	-----	---	1.4	2.48	-----	2.0
.002	.5	.885	11.49	0.00408	0.490	No	2.8	2.48	0.850	3.6
.002	.5	1.33	16.16	.00328	.610	Yes	.8	1.06	.242	2.0
.002	.5	1.77	20.86	.00238	.840	Yes	.6	1.06	.429	1.3
.002	1.0	.885	9.27	.00577	.347	No	2.8	2.48	.850	4.2
.002	1.0	1.33	12.73	.00471	.424	No	2.4	3.19	.961	3.7
.002	1.0	1.77	16.28	.00408	.490	Yes	1.2	2.12	.856	2.0
.002	1.5	.885	8.37	.00707	.283	No	3.2	2.84	.973	4.0
.002	1.5	1.33	11.40	.00576	.347	No	2.7	3.59	1.08	3.3
.003	.5	.885	18.36	.00408	.735	No	1.9	1.68	.575	2.6
.003	.5	1.33	28.41	.00328	.915	Yes	.9	1.20	.360	1.4
.003	.5	1.77	38.94	.00238	1.26	Yes	.6	1.06	.429	1.1
.003	1.0	.885	14.66	.00577	.520	No	2.6	2.30	.788	3.5
.003	1.0	1.33	20.71	.00471	.637	No	1.6	2.13	.642	2.3
.003	1.0	1.77	26.83	.00408	.735	Yes	1.1	1.95	.785	1.7
.003	1.5	.885	12.81	.00707	.424	No	2.6	2.30	.787	3.7
.003	1.5	1.33	17.97	.00576	.520	No	2.1	2.79	.840	2.6
.005	.5	.885	44.94	.00408	1.74	Yes	.5	.443	.151	.9
.005	.5	1.33	73.21	.00328	2.13	Yes	.5	.665	.200	.7
.005	.5	1.77	92.74	.00238	2.45	Yes	.5	.885	.357	.7
.005	1.0	.885	28.62	.00577	1.00	Yes	1.1	1.06	.334	1.6
.005	1.0	1.33	44.74	.00471	1.22	Yes	1.1	1.46	.440	1.3
.005	1.0	1.77	63.58	.00408	1.41	Yes	1.1	1.95	.786	1.3
.005	1.5	.885	24.27	.00707	.775	Yes	1.7	1.50	.515	2.2
.005	1.5	1.33	35.10	.00576	.950	Yes	1.6	2.13	.640	1.9

TABLE I.- PRESENTATION OF RESULTS - Concluded

(c) $\frac{u'}{u}$ = 35.0 percent

k, in.	x_k, in.	$\frac{u_\infty}{\nu_\infty}$, per inch	$\sqrt{R_k}$	δ_k^*, in.	$\frac{k}{\delta_k^*}$	Transition at x_k	x_t, in.	R_t	$\frac{R_t}{R_{t,o}}$	x_t', in.
0	---	0.885×10^6	-----	-------	-----	---	2.7	2.39×10^6	-----	4.0
0	---	1.33	-----	-------	-----	---	2.1	2.79	-----	3.1
0	---	1.77	-----	-------	-----	---	1.4	2.48	-----	2.3
.002	.5	.885	11.49	0.00408	0.490	No	2.25	1.99	0.833	2.9
.002	.5	1.33	16.16	.00328	.610	Yes	.8	1.06	.391	1.5
.002	.5	1.77	20.86	.00238	.840	Yes	.6	1.06	.429	1.1
.002	1.0	.885	9.27	.00577	.347	No	2.6	2.30	.961	3.6
.002	1.0	1.33	12.73	.00471	.424	No	2.1	2.79	1.00	2.9
.002	1.0	1.77	16.28	.00408	.490	Yes	1.2	2.12	.858	2.0
.002	1.5	.885	8.37	.00707	.283	No	2.6	2.30	.962	4.3
.002	1.5	1.33	11.40	.00576	.347	No	2.1	2.79	1.00	3.0
.003	.5	.885	18.36	.00408	.735	No	1.1	.98	.410	2.0
.003	.5	1.33	28.41	.00328	.915	Yes	.6	.8	.286	1.1
.003	.5	1.77	38.94	.00238	1.26	Yes	.6	1.06	.429	1.1
.003	1.0	.885	14.66	.00577	.520	No	2.2	1.95	.815	3.2
.003	1.0	1.33	20.71	.00471	.637	Yes	1.3	1.73	.619	2.2
.003	1.0	1.77	26.83	.00408	.735	Yes	1.2	2.12	.859	1.7
.003	1.5	.885	12.81	.00707	.424	No	2.7	2.39	1.00	3.8
.003	1.5	1.33	17.97	.00576	.520	No	1.8	2.39	.856	2.5
.005	.5	.885	44.94	.00408	1.74	Yes	.6	.53	.222	1.2
.005	.5	1.33	73.21	.00328	2.13	Yes	.6	.8	.286	.9
.005	.5	1.77	92.74	.00238	2.45	Yes	.6	1.06	.429	.9
.005	1.0	.885	28.62	.00577	1.00	Yes	1.1	.98	.408	1.6
.005	1.0	1.33	44.74	.00471	1.22	Yes	1.1	1.46	.524	1.6
.005	1.0	1.77	63.58	.00408	1.41	Yes	1.1	1.95	.788	1.5
.005	1.5	.885	24.27	.00707	.775	Yes	1.8	1.59	.667	2.5
.005	1.5	1.33	35.10	.00576	.950	Yes	1.6	2.13	.762	2.2

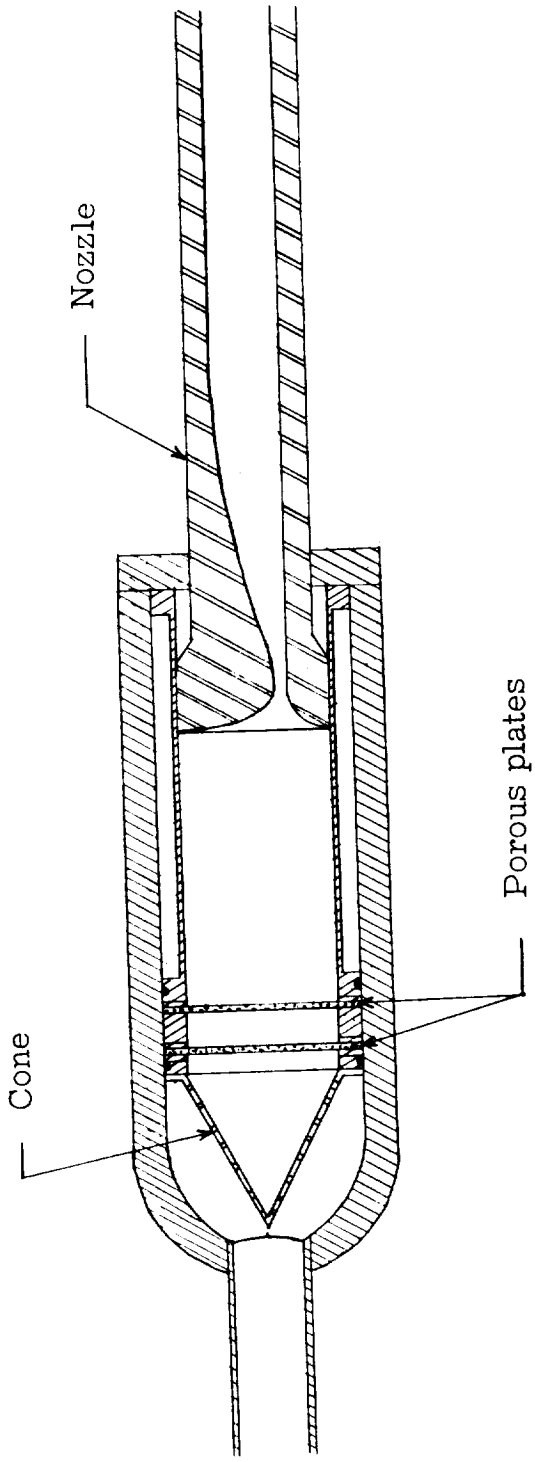

Figure 1.- Sketch of settling chamber and nozzle.

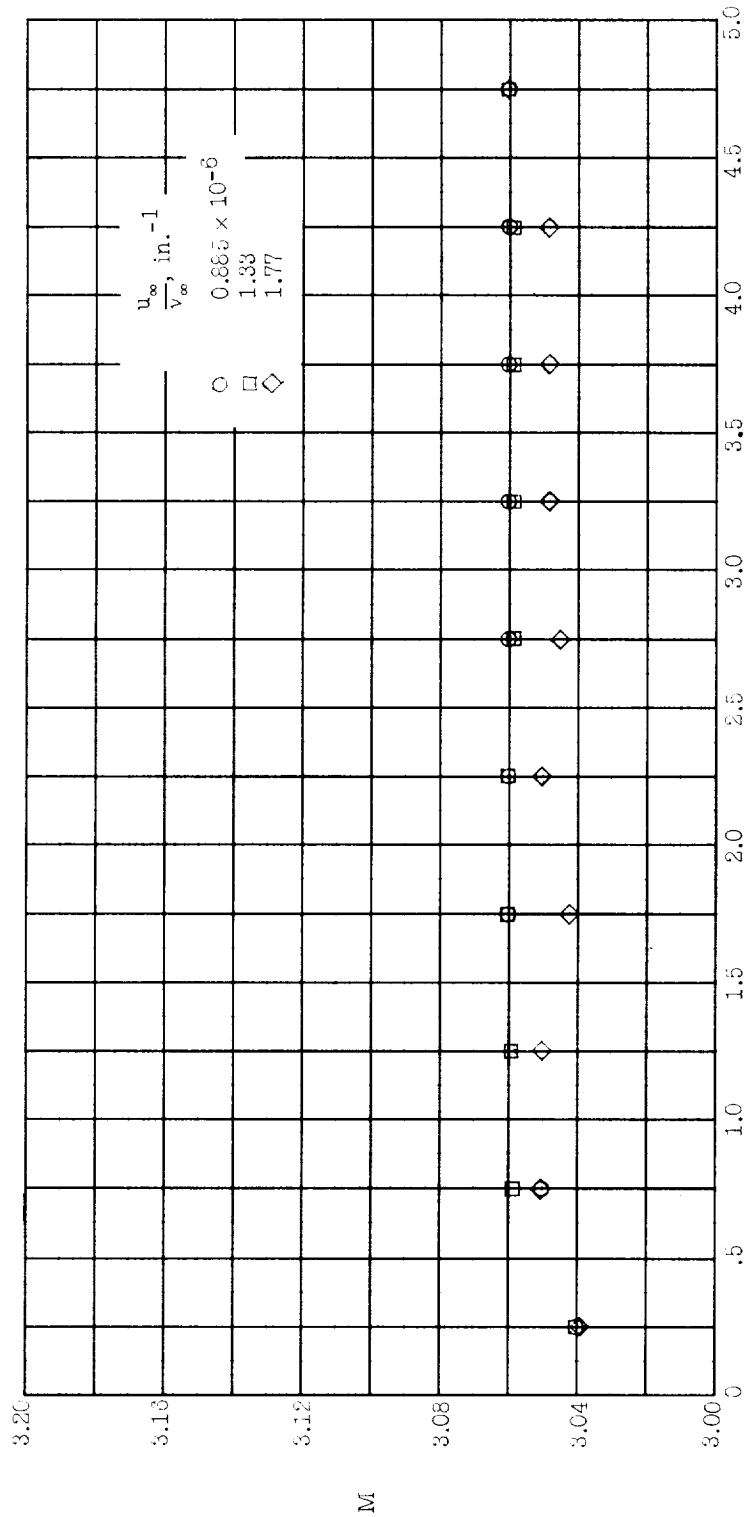

Figure 2.- Variation of Mach number along the forward portion of the plate.

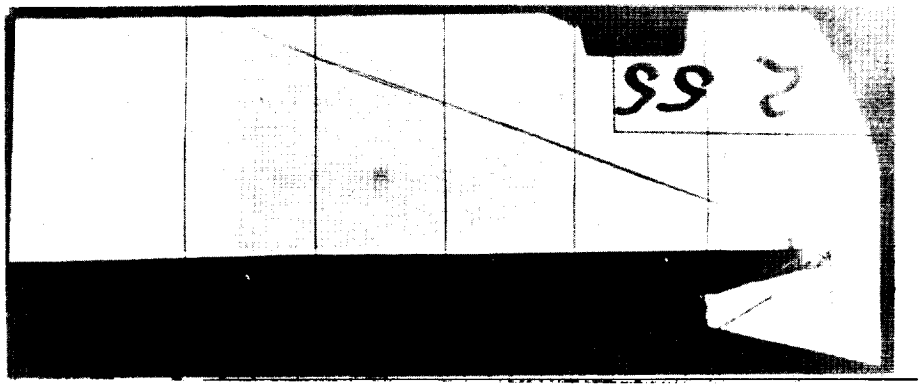

(a) $\frac{u_\infty}{\nu_\infty} = 0.885 \times 10^6$ in.$^{-1}$.

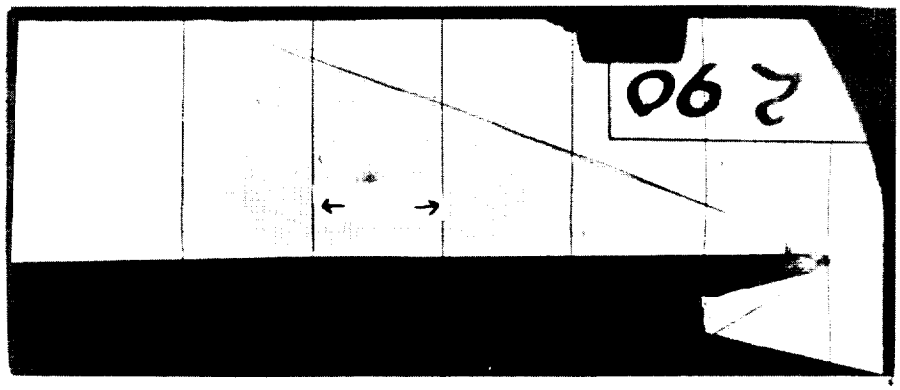

(b) $\frac{u_\infty}{\nu_\infty} = 1.33 \times 10^6$ in.$^{-1}$.

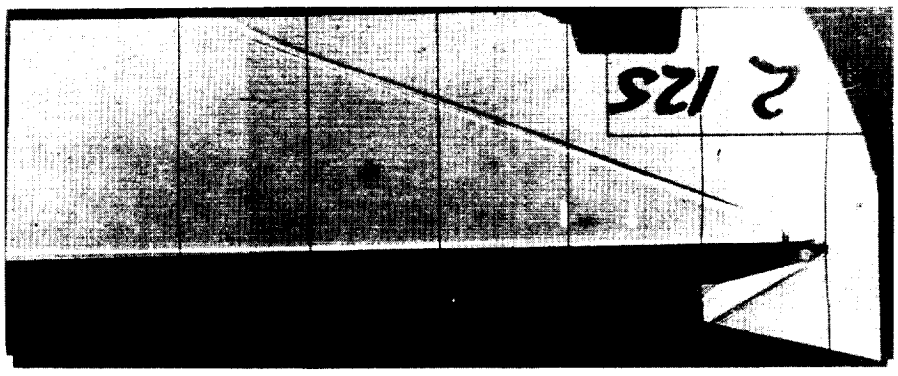

(c) $\frac{u_\infty}{\nu_\infty} = 1.77 \times 10^6$ in.$^{-1}$. L-58-140a

Figure 3.- Shadowgraph indication of transition. Smooth plate; $\frac{u'}{u} = 35$ percent. Arrows indicate beginning of transition.

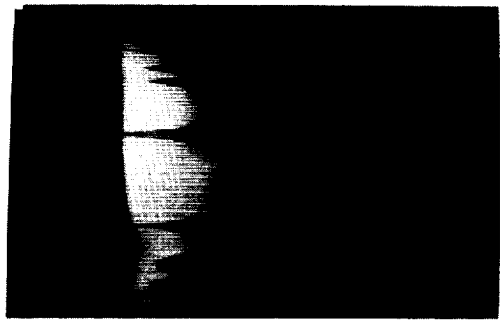

(a) $\frac{u_\infty}{\nu_\infty} = 0.885 \times 10^6$ in.$^{-1}$.

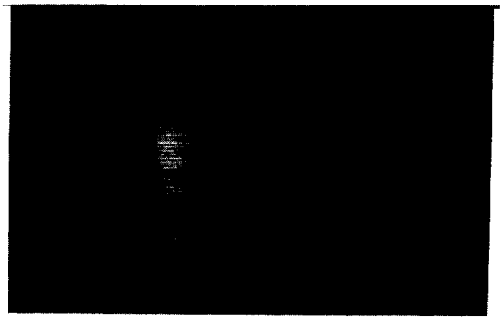

(b) $\frac{u_\infty}{\nu_\infty} = 1.33 \times 10^6$ in.$^{-1}$.

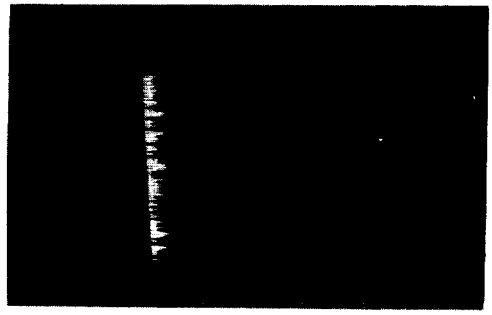

(c) $\frac{u_\infty}{\nu_\infty} = 1.77 \times 10^6$ in.$^{-1}$. L-58-141a

Figure 4.- Transition patterns by sublimating solid. White portion is laminar. k = 0.002 in.; x_k = 0.5 in.

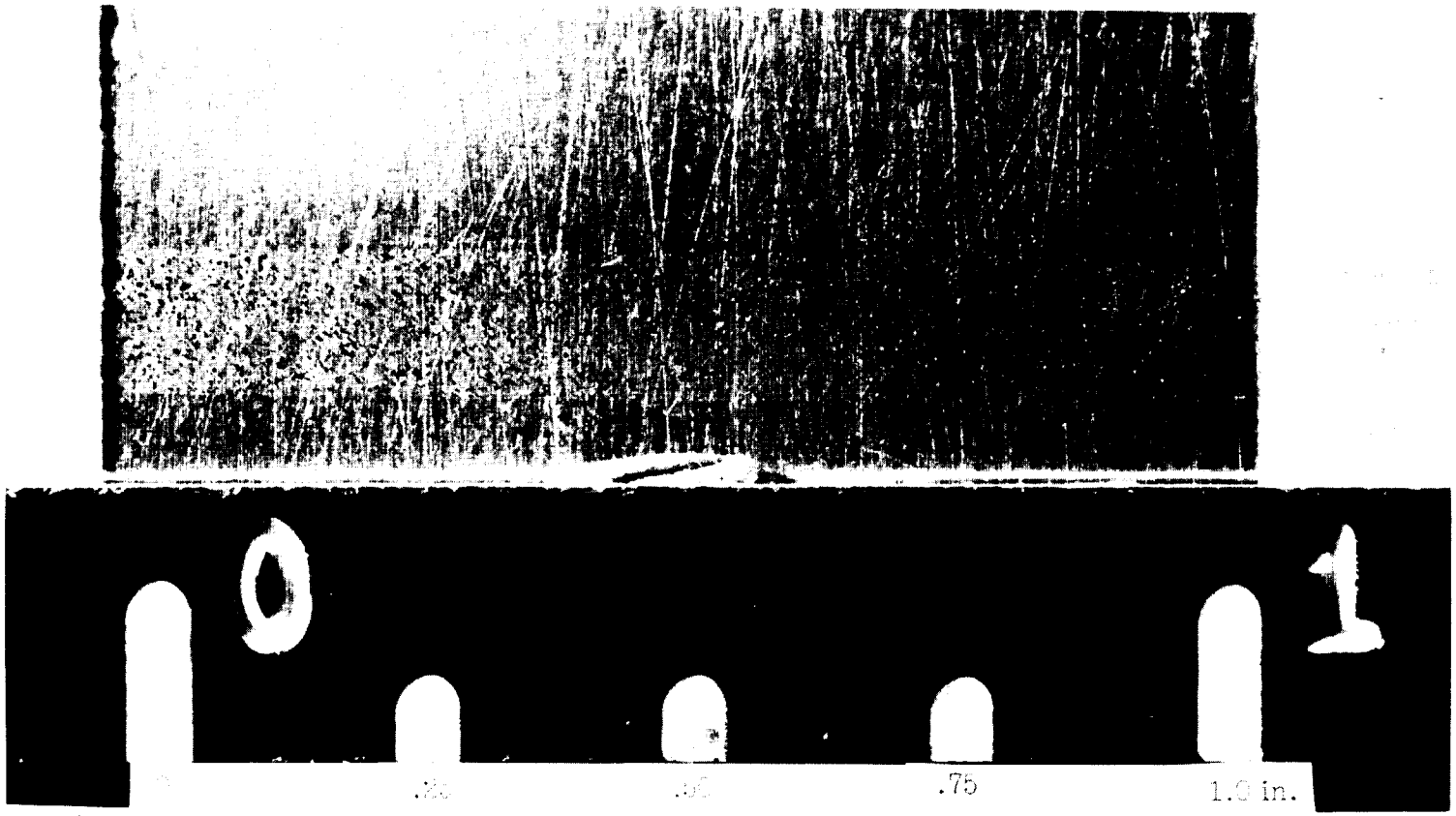

(a) k = 0.002 inch. L-58-978.1

Figure 5.- Photographs of roughness.

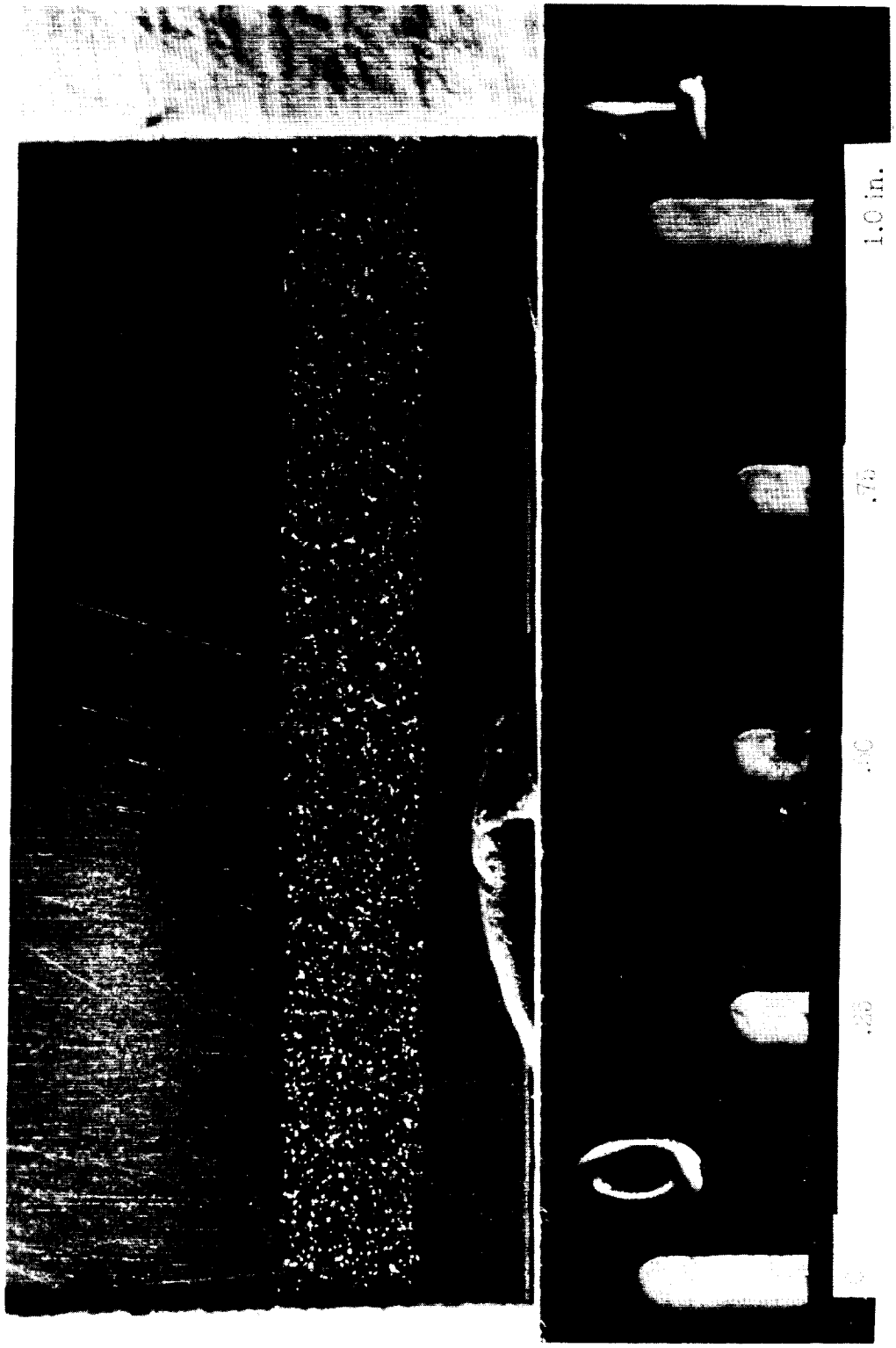

(b) k = 0.003 inch. L-58-979.1

Figure 5.- Continued.

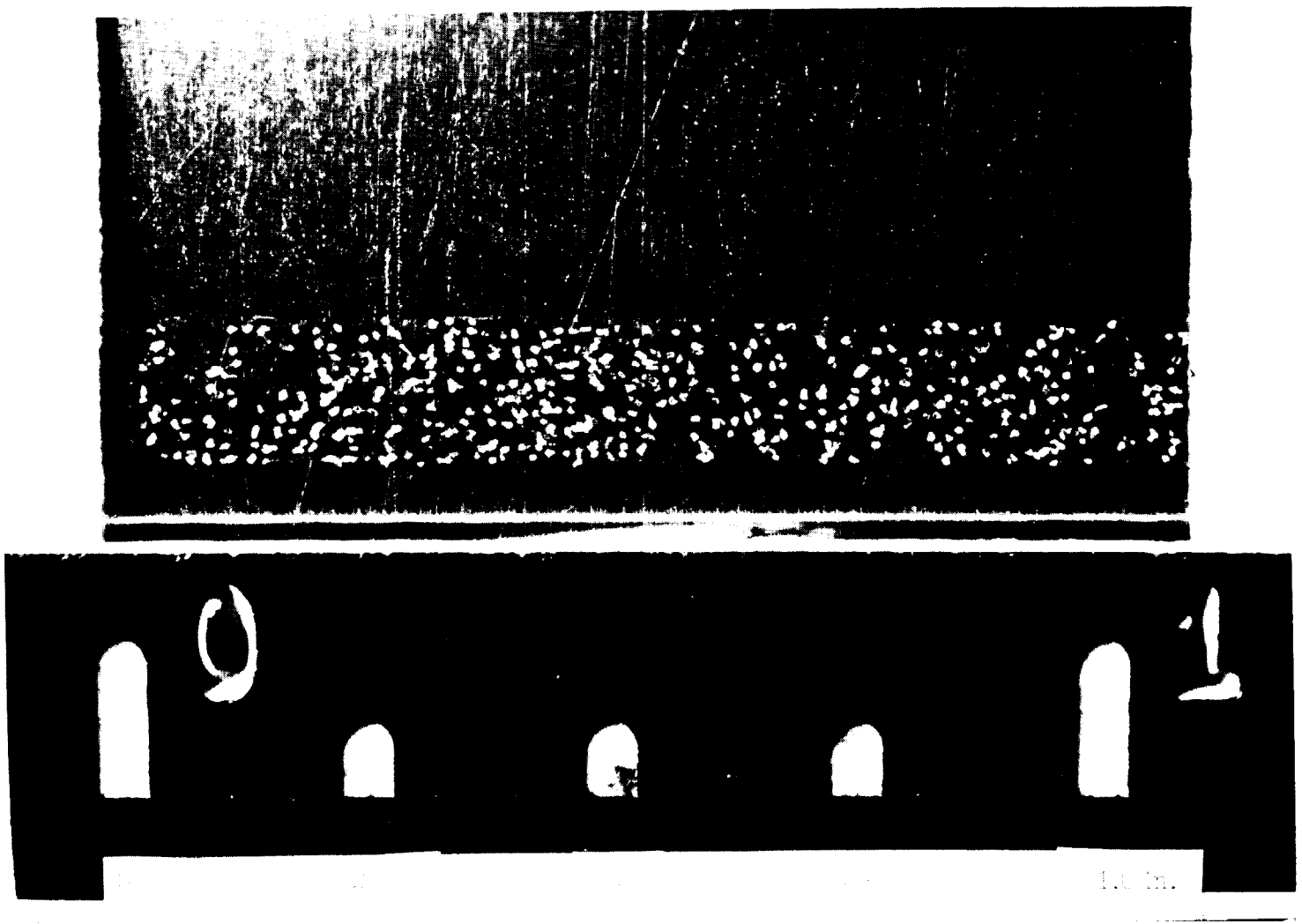

(c) k = 0.005 inch. L-58-977.1

Figure 5.- Concluded.

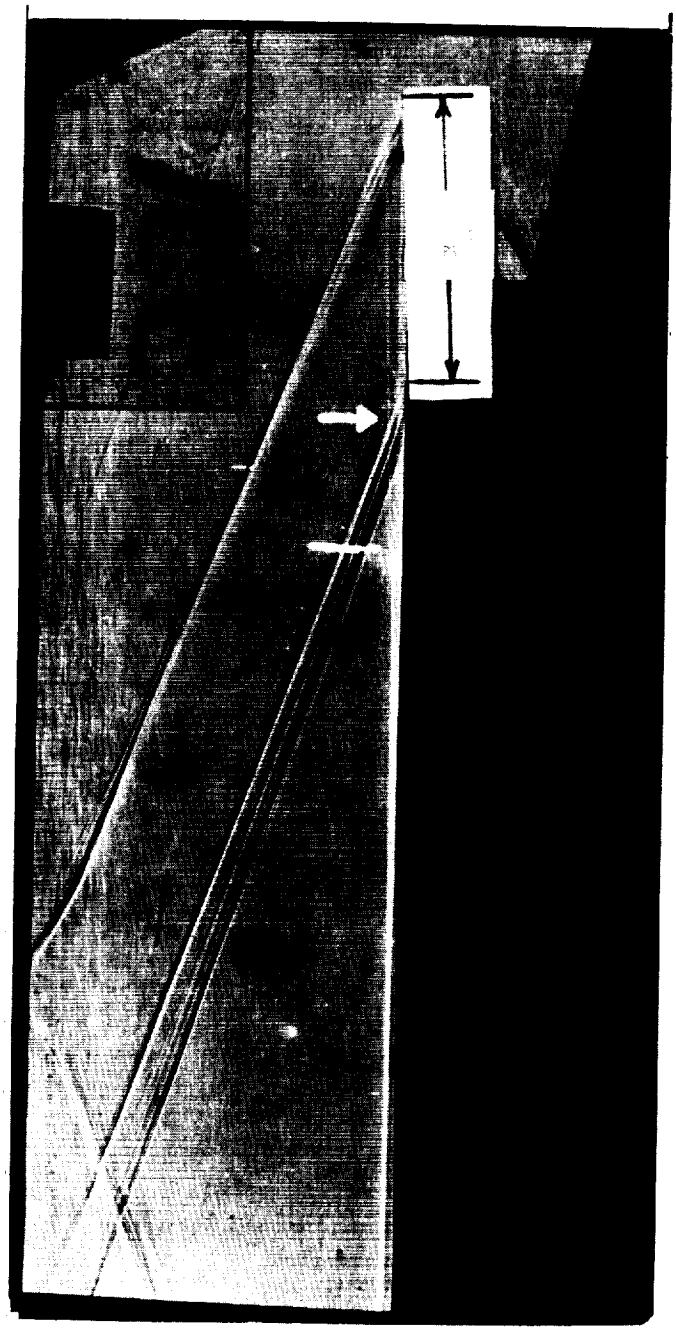

L-58-142a

Figure 6.- Intersection of white laminar line by disturbance waves from roughness. $k = 0.002$ inch; $x_k = 1.5$ inch; $\frac{u_\infty}{\nu_\infty} = 1.77 \times 10^6$ in.$^{-1}$; arrow indicates beginning of transition.

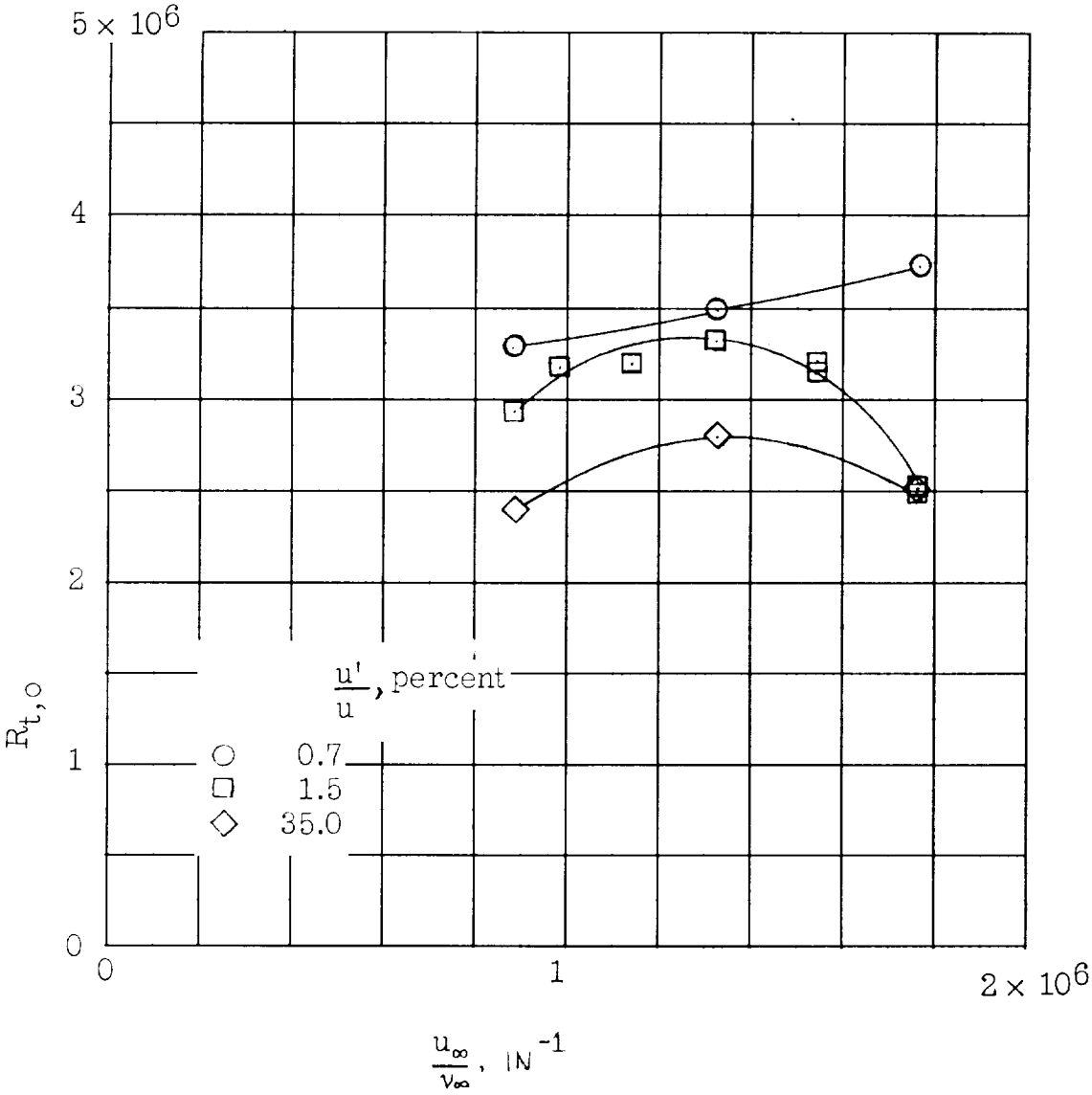

Figure 7.- Transition Reynolds number variation with unit Reynolds number on the smooth plate at different turbulence levels.

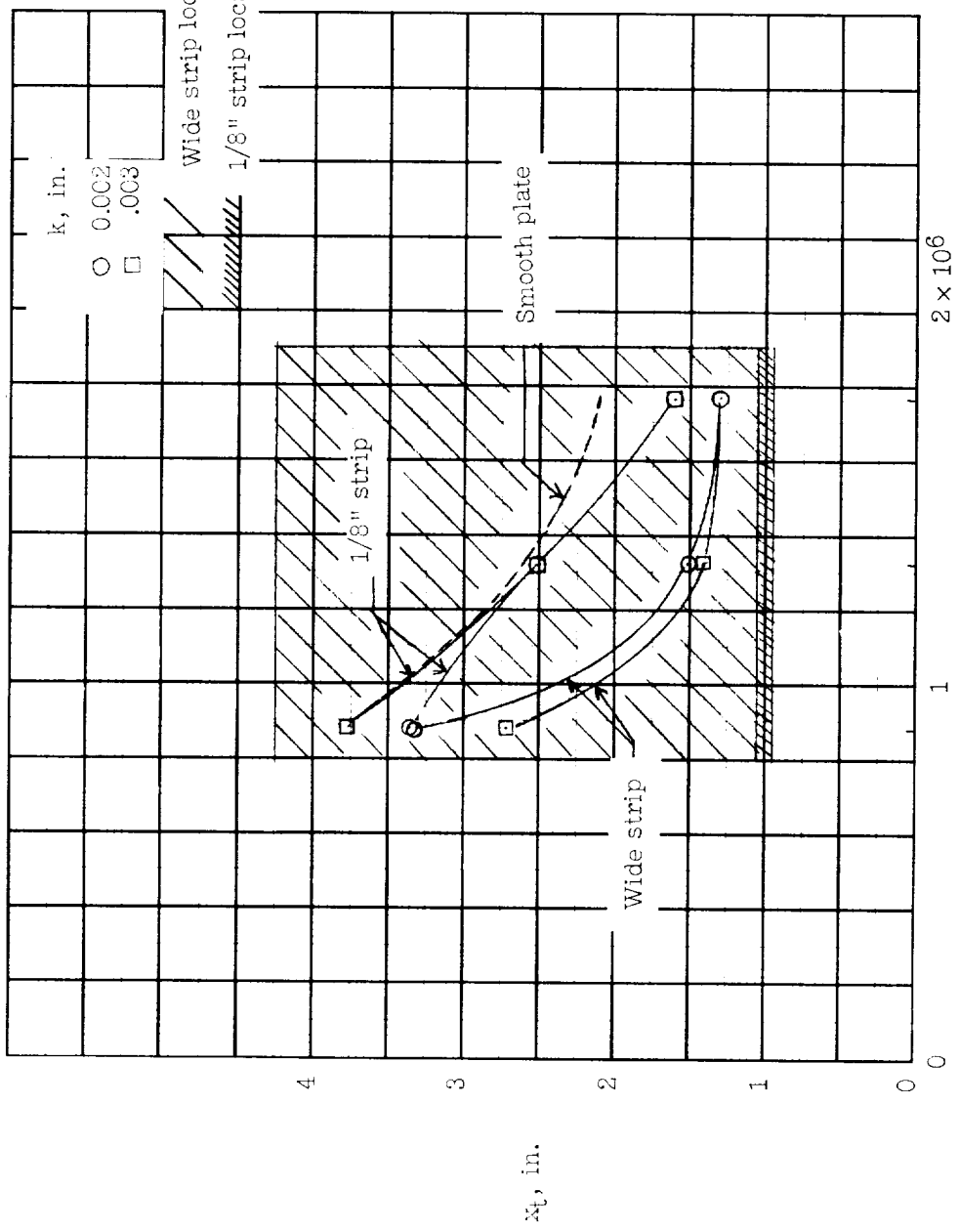

Figure 8.- Effect of width of roughness strip on transition. $\frac{u'}{u} = 0.7$ percent.

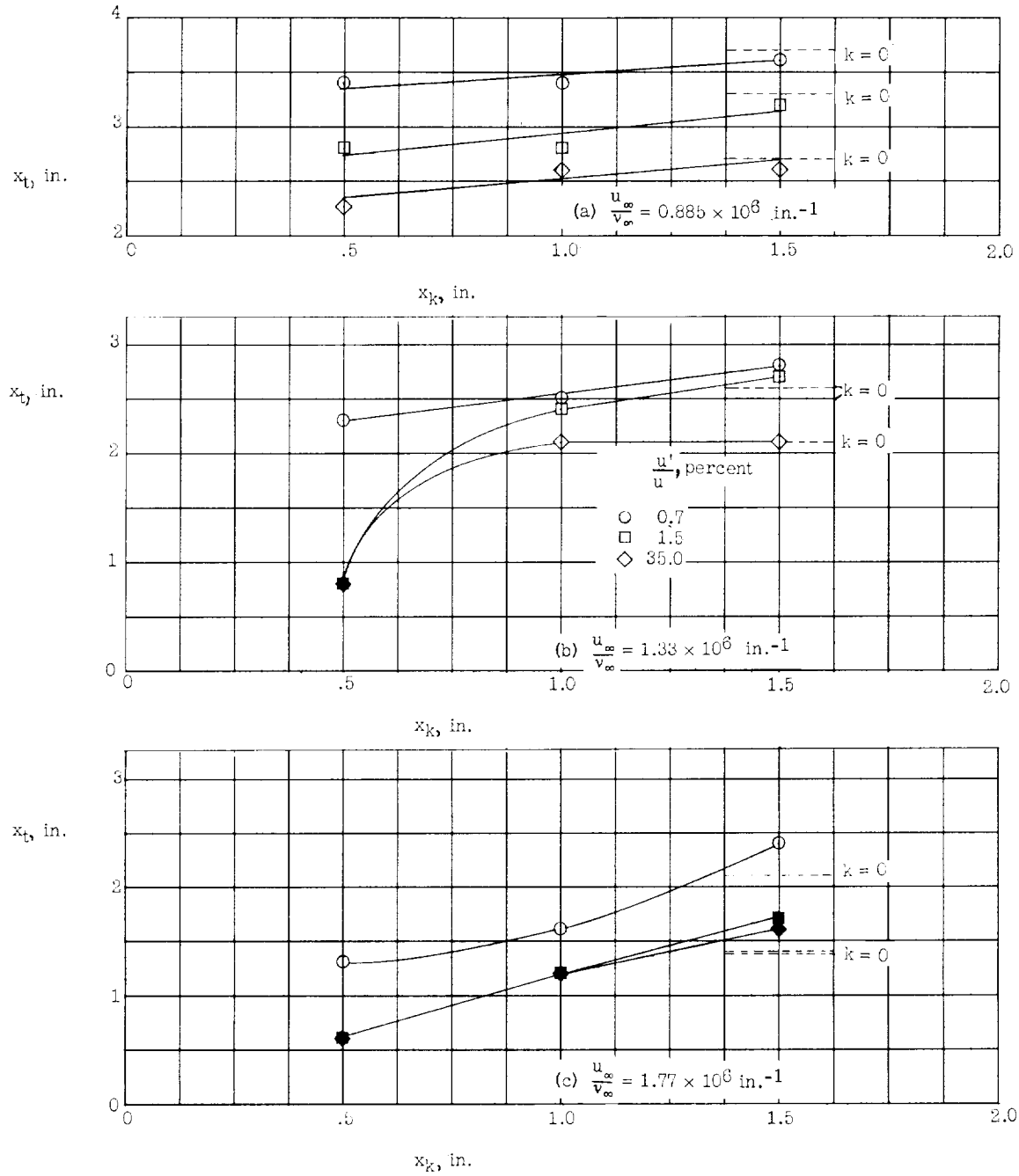

Figure 9.- Variation of transition location with roughness location for a roughness height of 0.002 inch and different turbulence levels. Solid symbols denote transition essentially at roughness.

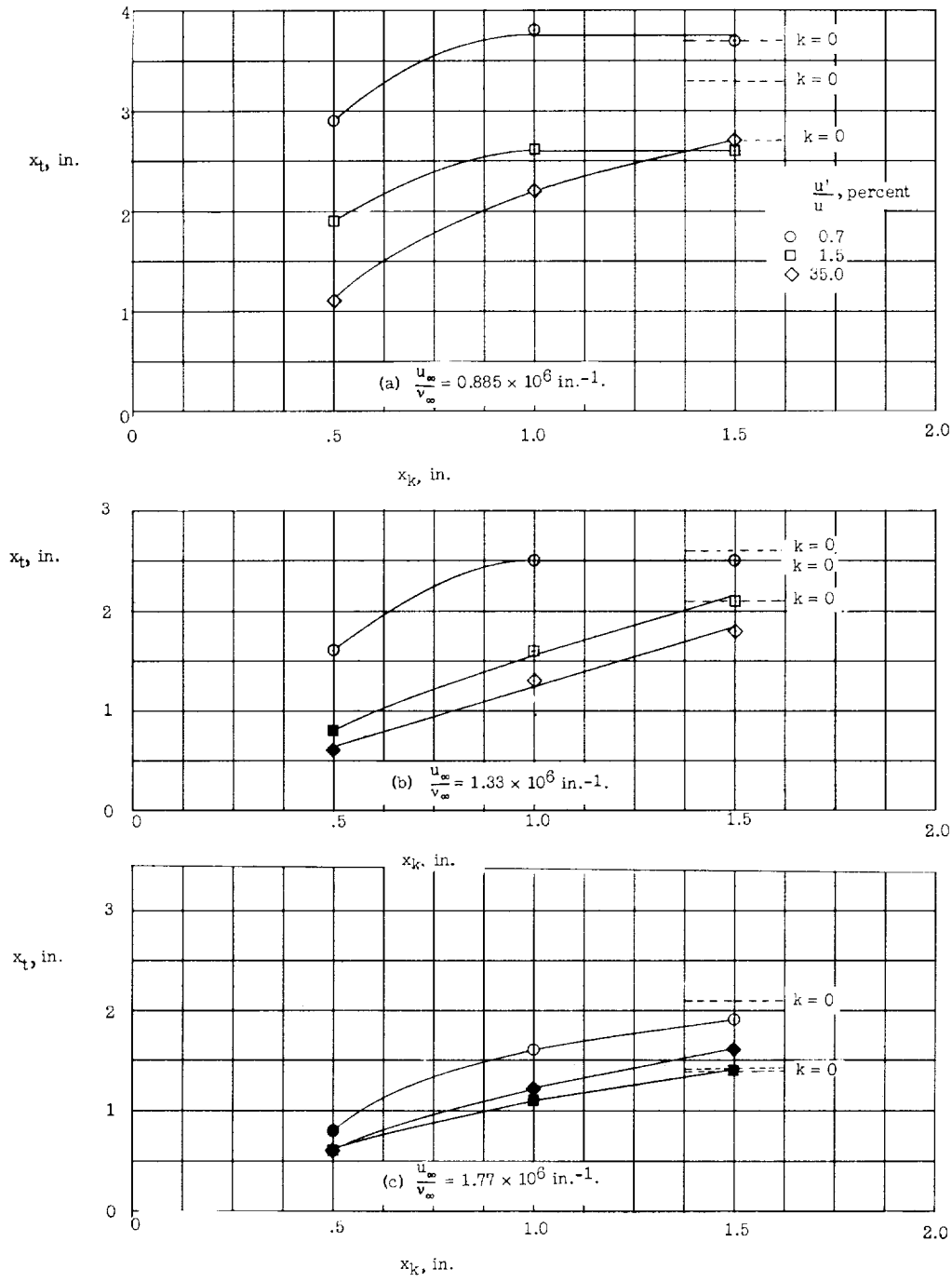

Figure 10.- Variation of transition location with roughness location for a roughness height of 0.003 inch and different turbulence levels. Solid symbols denote transition essentially at roughness.

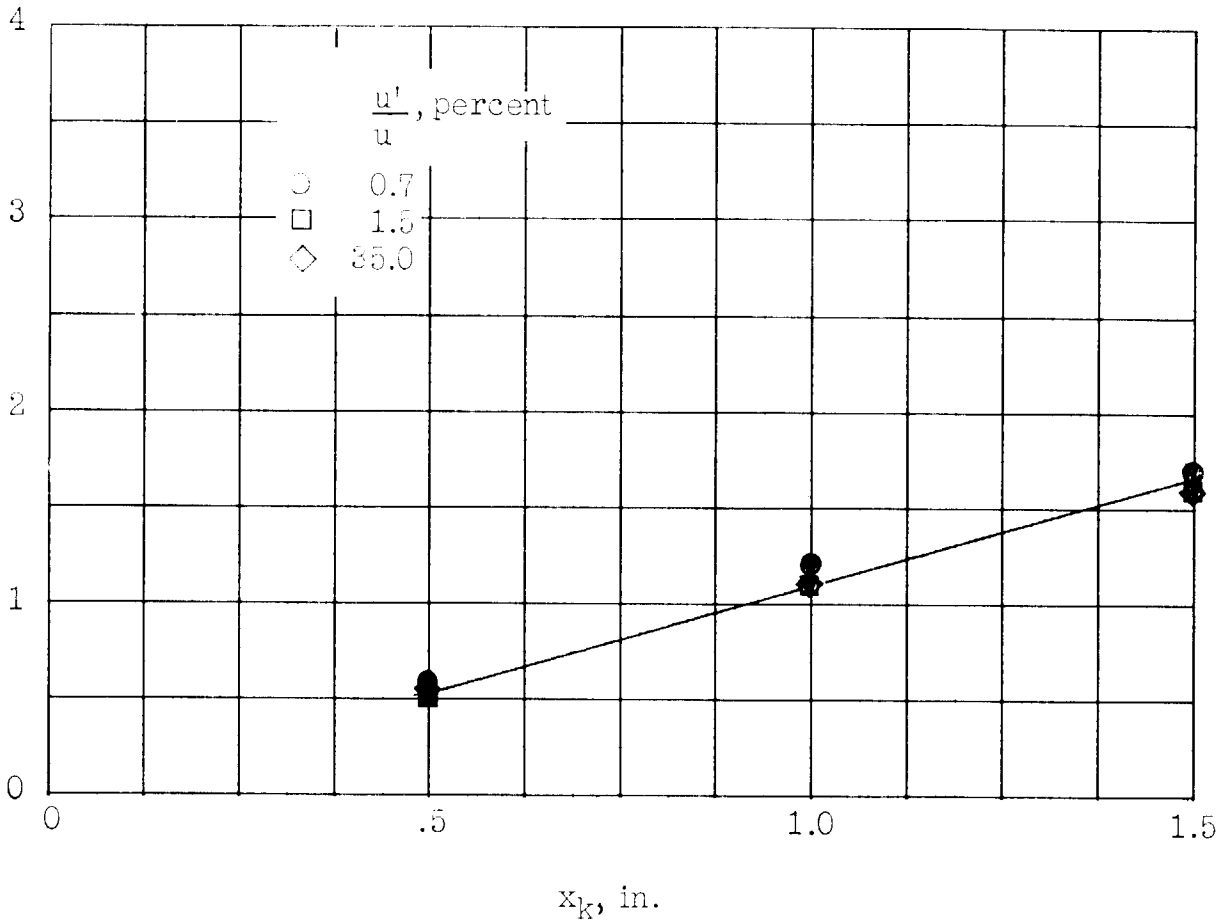

Figure 11.- Variation of transition location with roughness location for a roughness height of 0.005 inch and different turbulence levels. Solid symbols denote transition essentially at roughness. Data are the same for $\frac{u_\infty}{\nu_\infty} = 0.885$, 1.33, and 1.77×10^6 in.$^{-1}$.

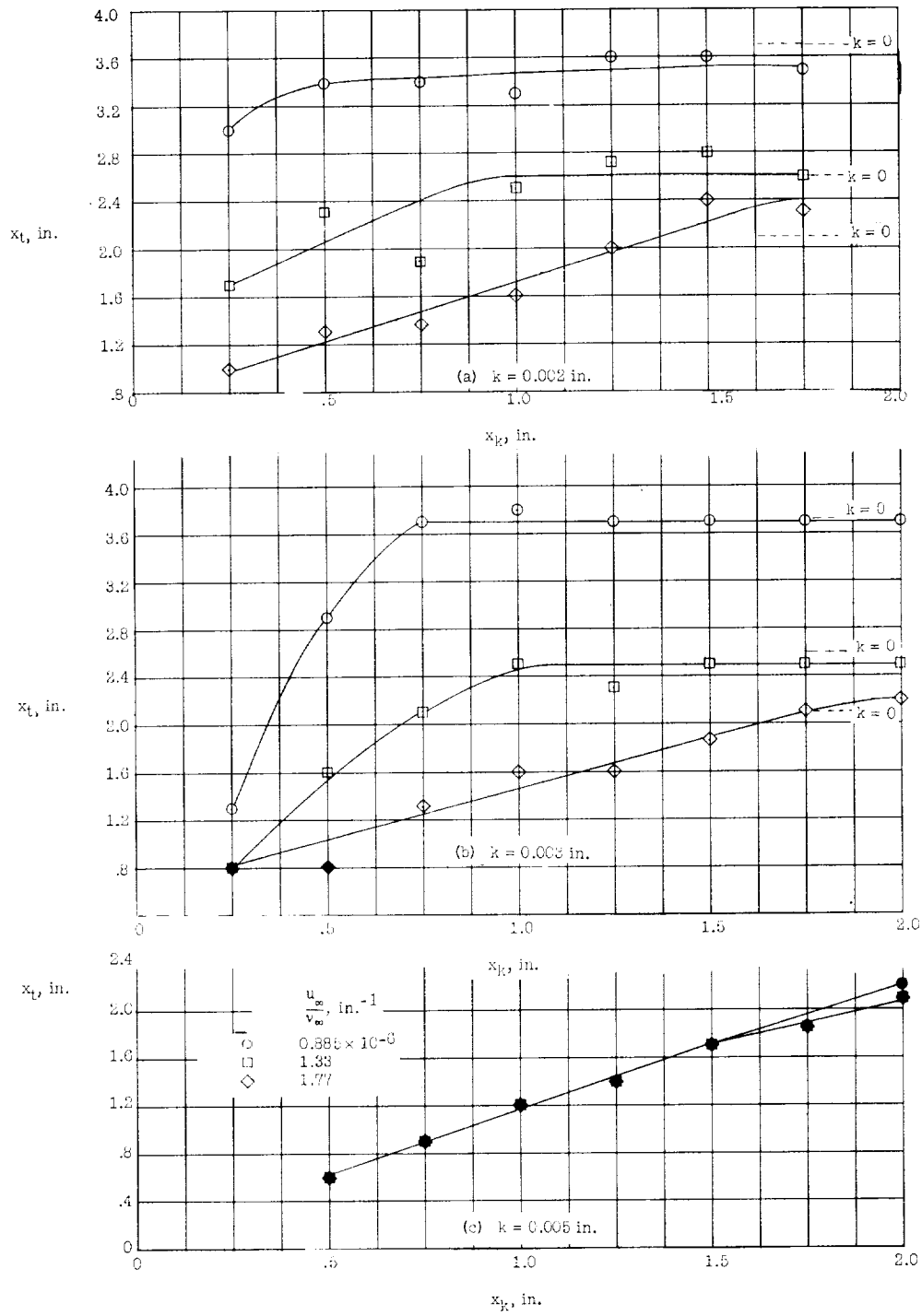

Figure 12.- Variation of transition location with roughness location for different Reynolds numbers at the low turbulence level.

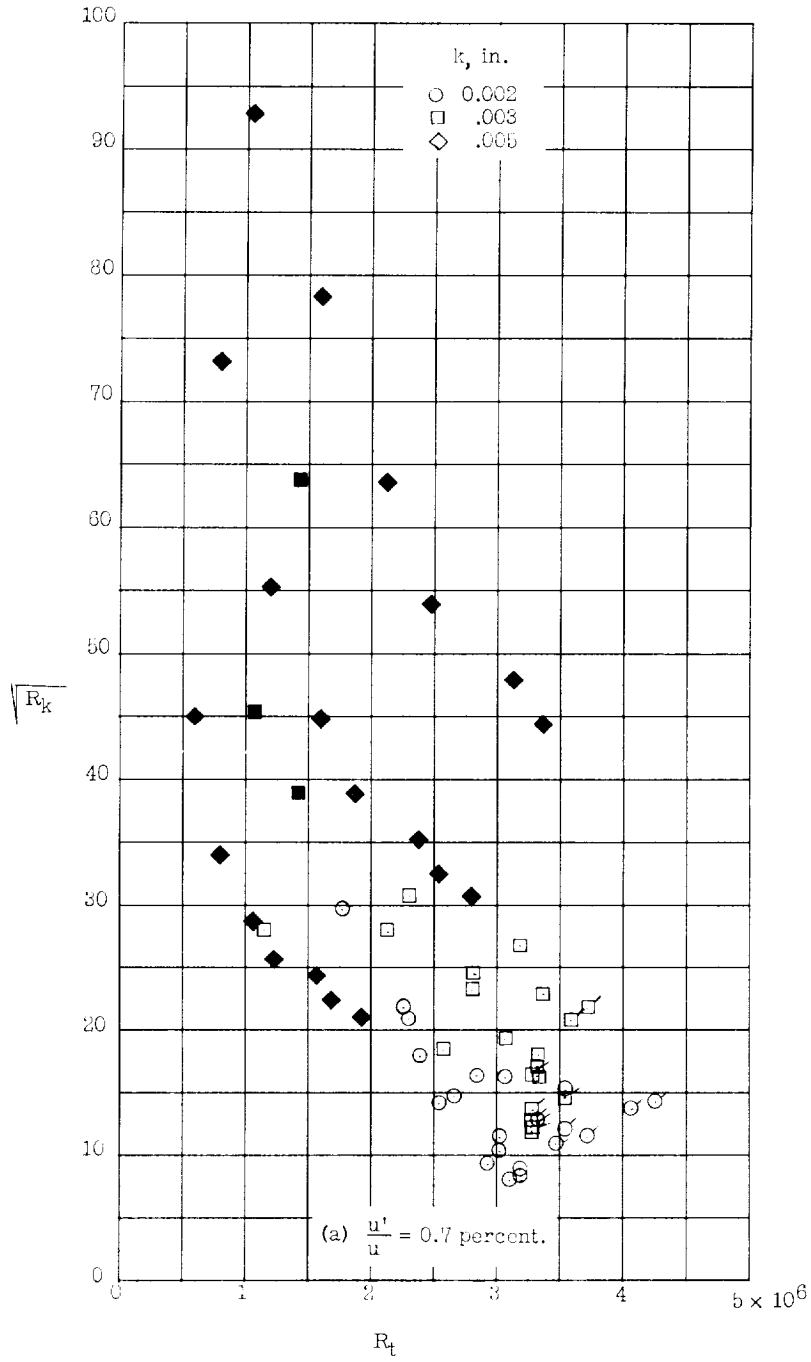

Figure 13.- Variation of roughness Reynolds number with transition Reynolds number for different roughness heights. Solid symbols denote transition essentially at roughness. Flagged symbols denote transition not moved forward by roughness.

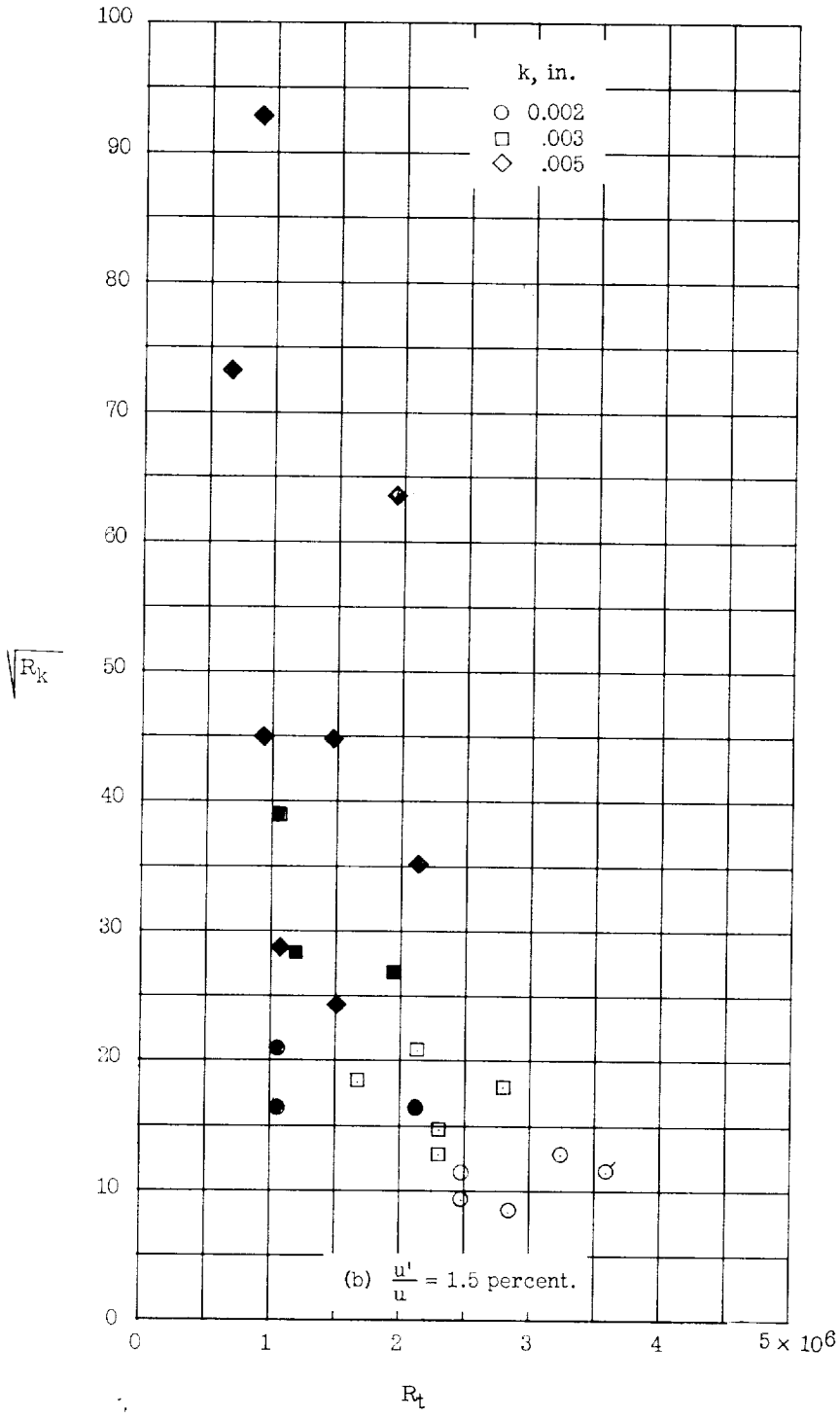

Figure 13.- Continued.

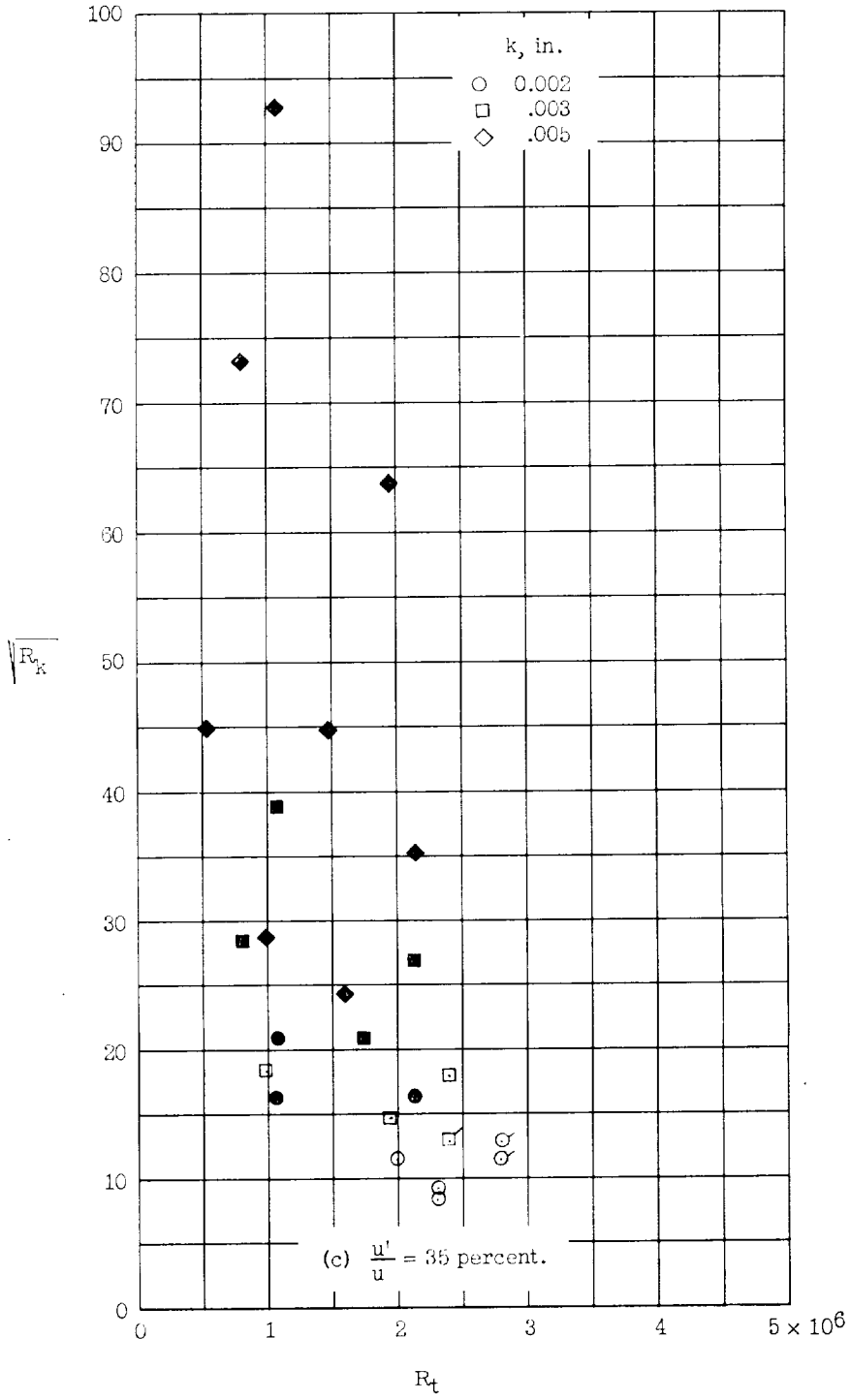

Figure 13.- Concluded.

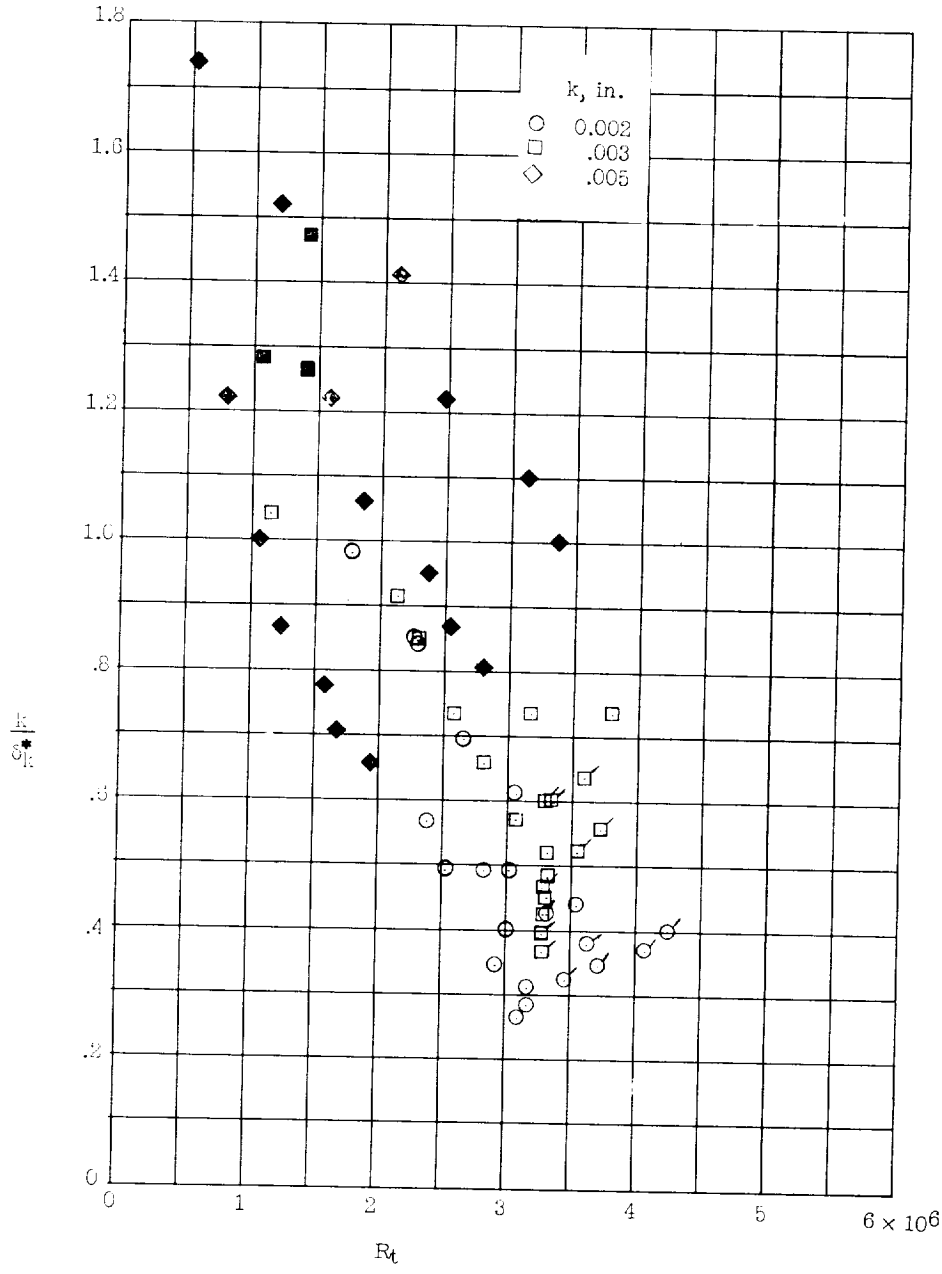

(a) $\frac{u'}{u}$ = 0.7 percent.

Figure 14.- Variation of transition Reynolds number with the low-speed roughness parameter for different roughness heights. Solid symbols indicate transition essentially at roughness. Flagged symbols denote transition not moved forward by roughness.

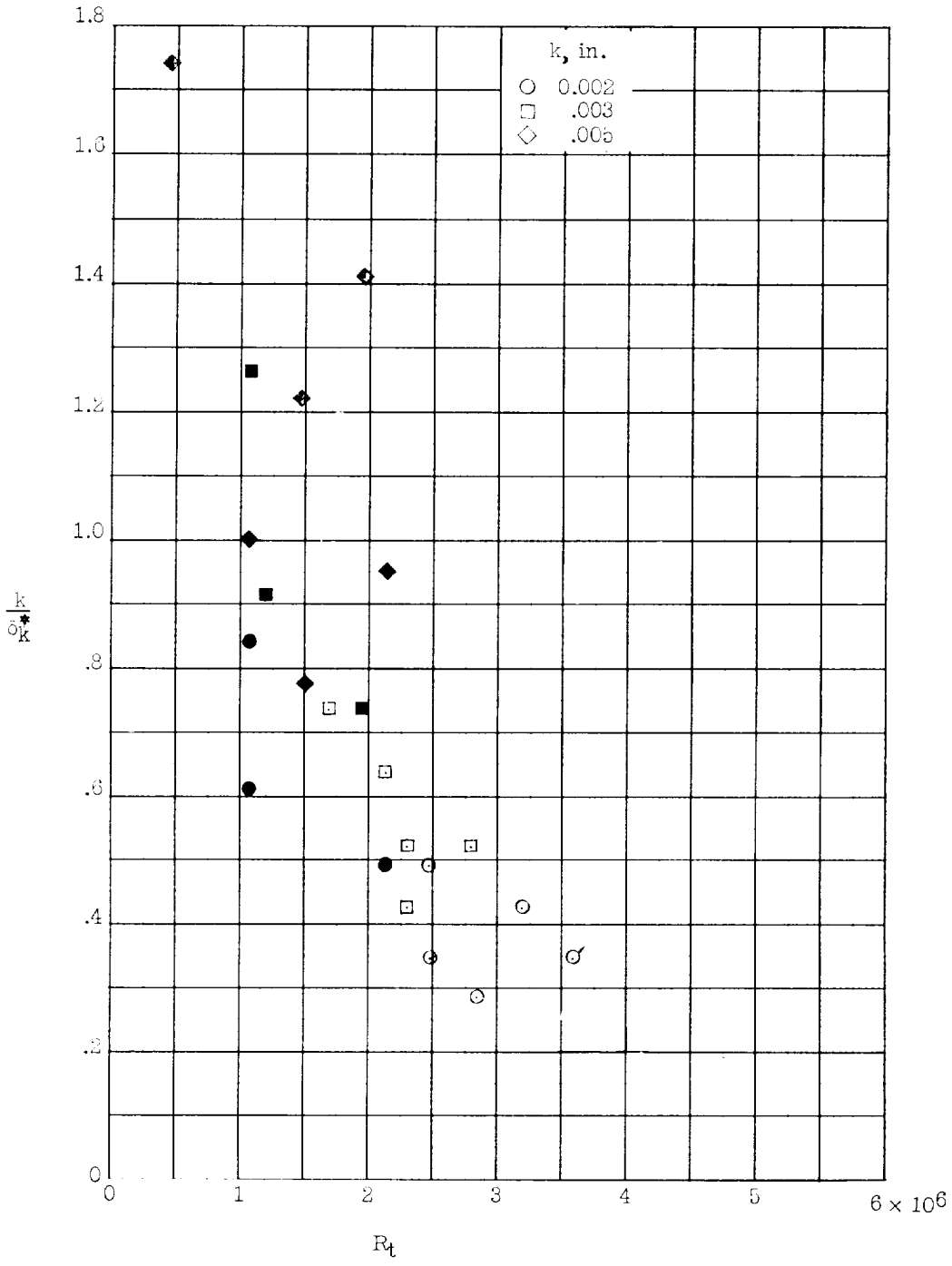

(b) $\frac{u'}{u}$ = 1.5 percent.

Figure 14.- Continued.

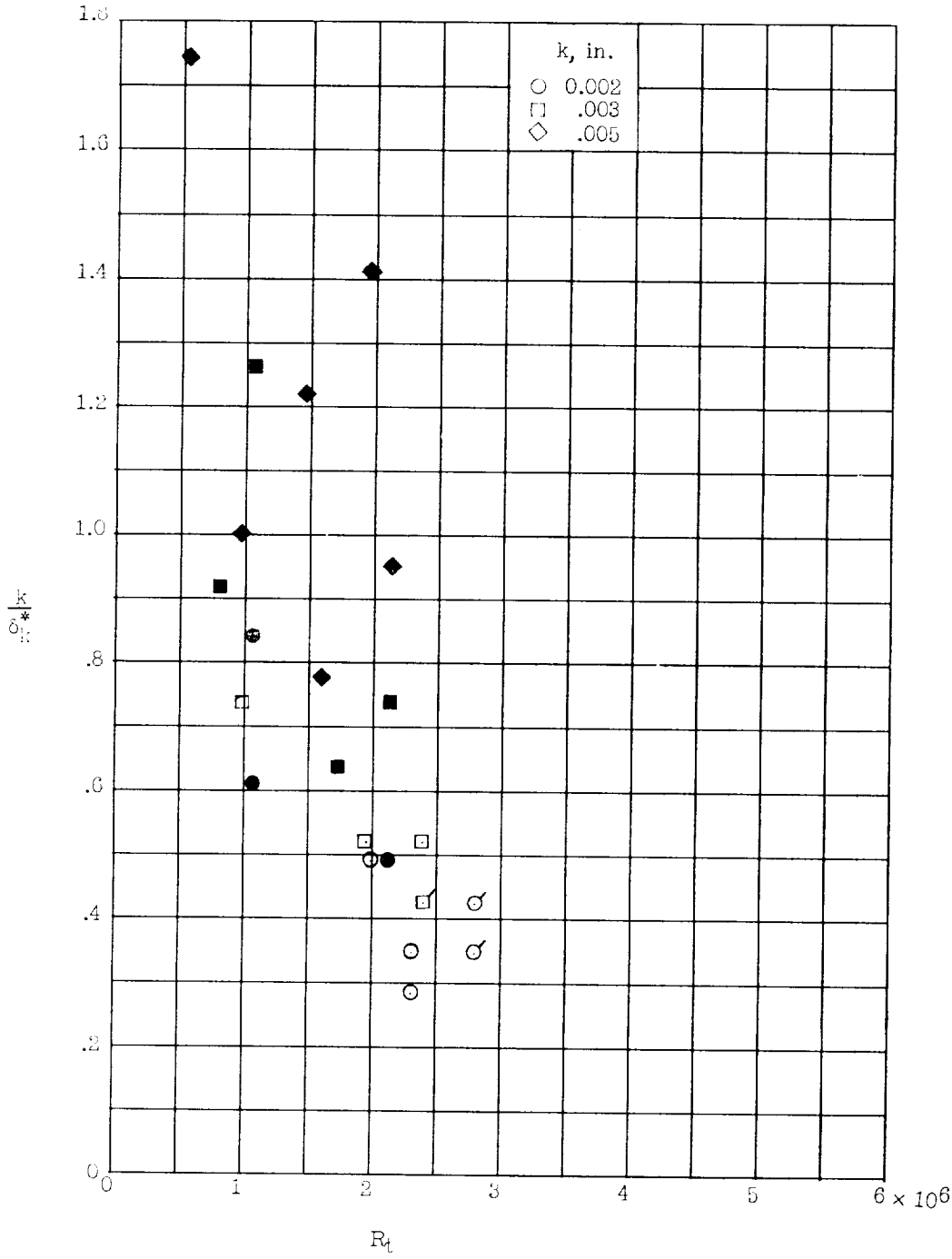

(c) $\frac{u'}{u}$ = 35 percent.

Figure 14.- Concluded.

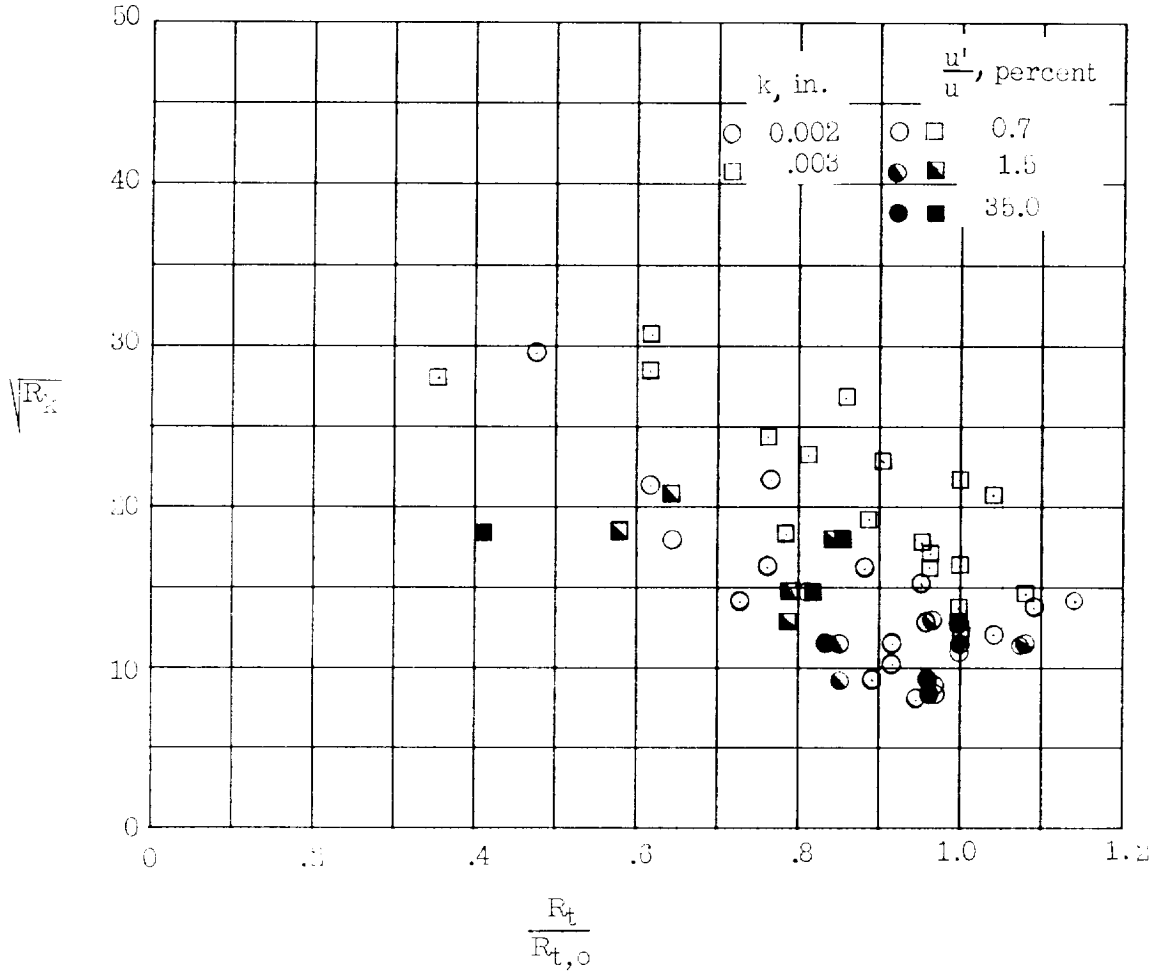

Figure 15.- Variation of transition Reynolds number ratio with roughness Reynolds number for different turbulence levels. Points for which transition is at roughness are not shown.

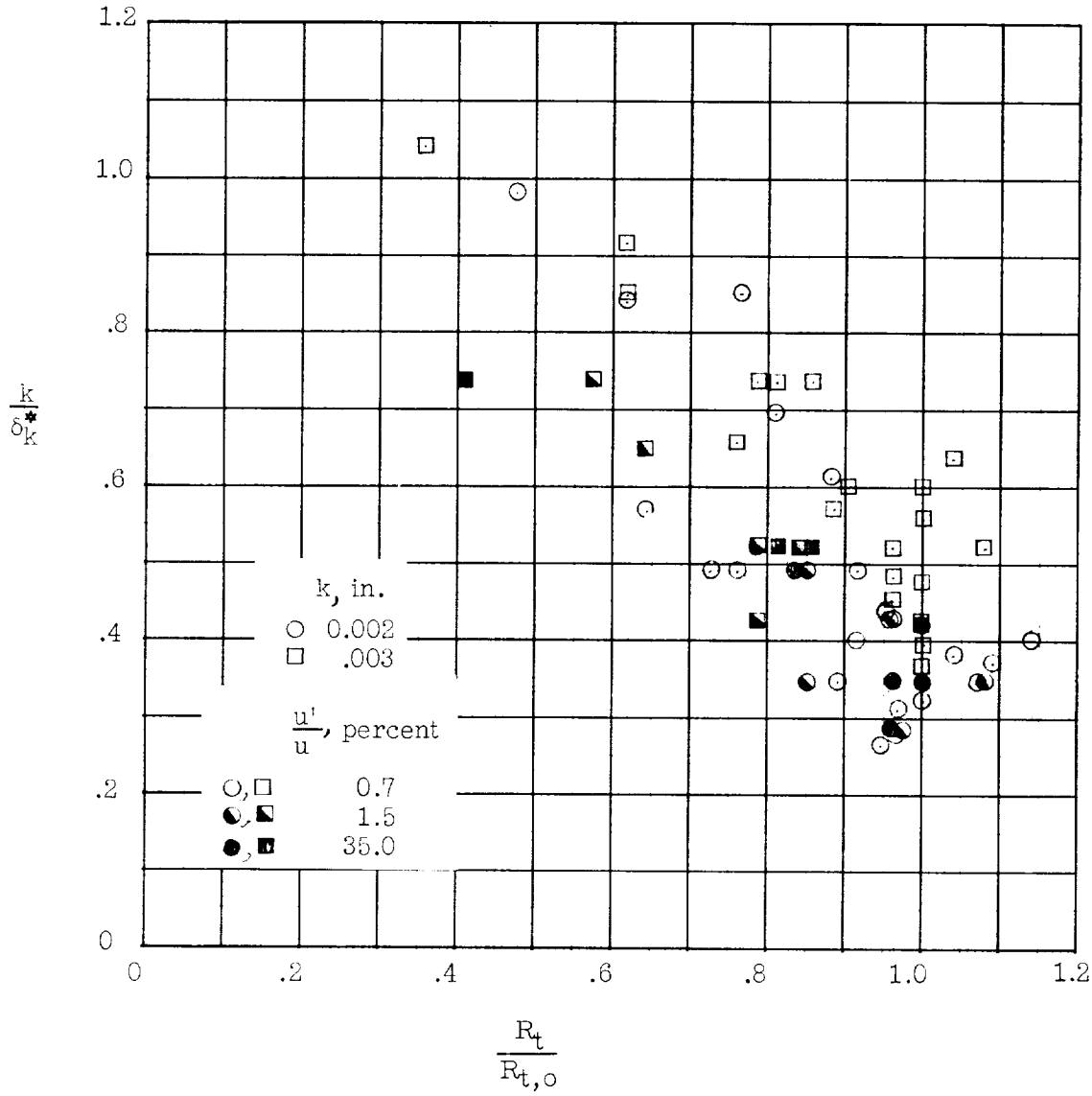

Figure 16.- Variation of Dryden's low-speed roughness parameter with transition Reynolds number ratio for different turbulence levels.

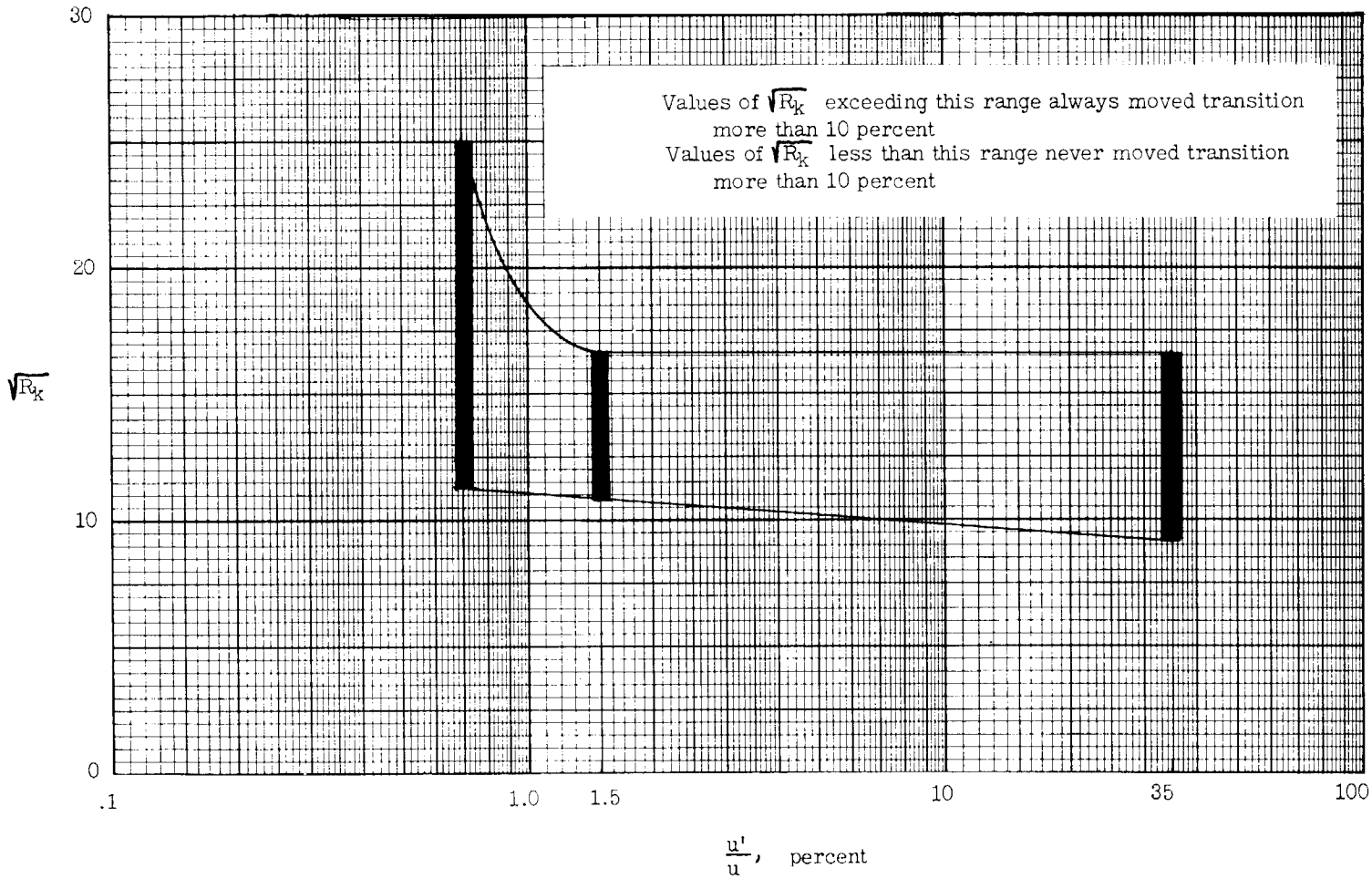

Figure 17.- Variation of range of roughness Reynolds number which may affect transition less than 10 percent with turbulence level.

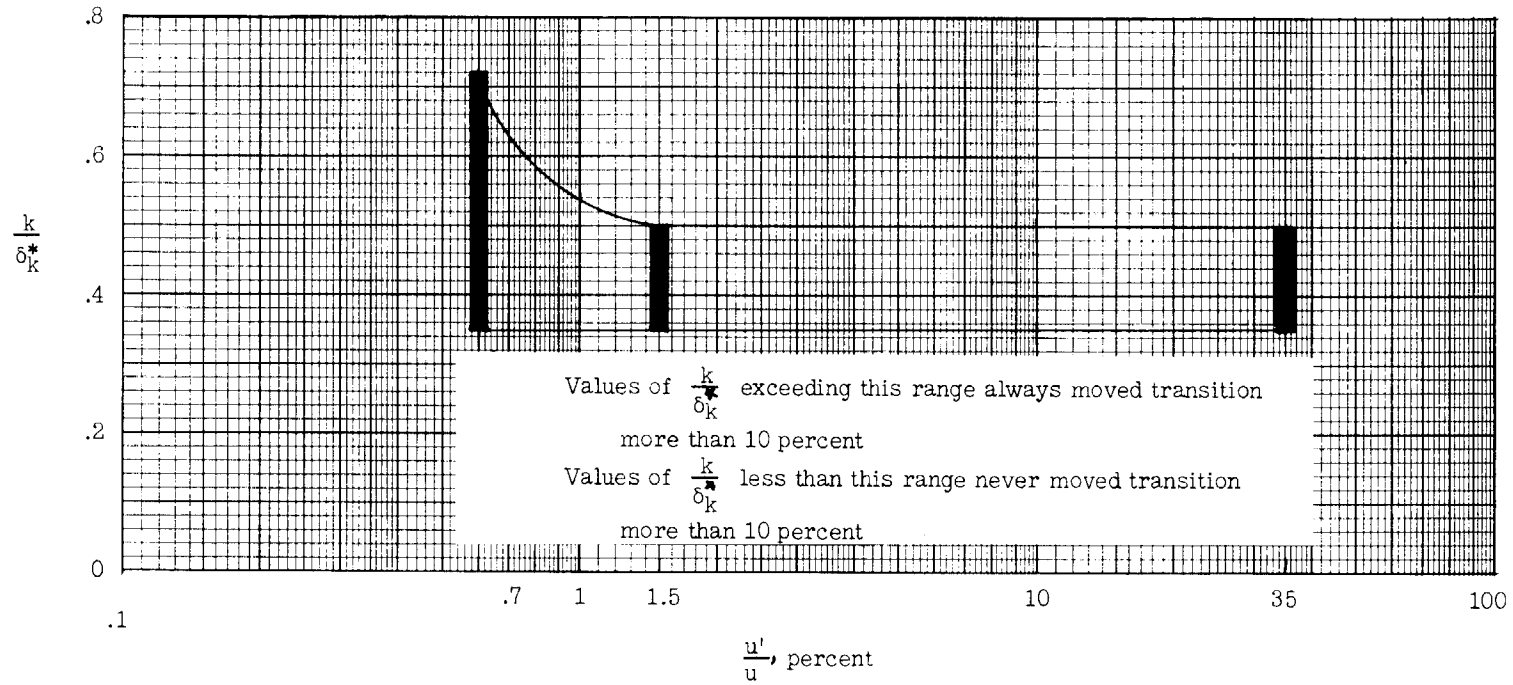

Figure 18.- Variation of range of Dryden's low-speed roughness parameter which may affect transition less than 10 percent with turbulence level.

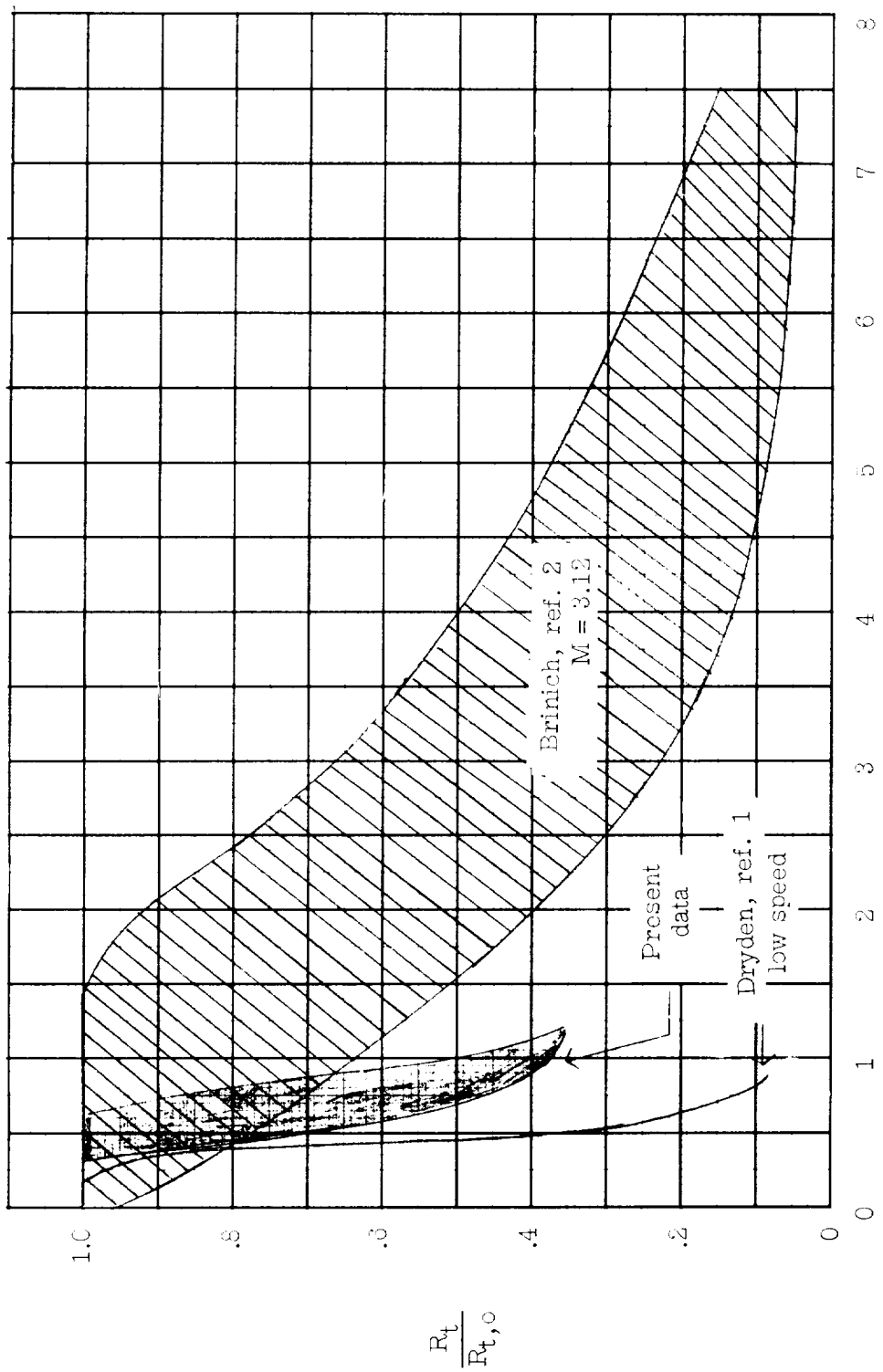

Figure 19.- Comparison of present results with results for two-dimensional data.

NASA - Langley Field, Va.

NASA MEMO 2-9-59L
National Aeronautics and Space Administration.
AN EXPERIMENTAL STUDY AT A MACH NUMBER OF 3 OF THE EFFECT OF TURBULENCE LEVEL AND SANDPAPER-TYPE ROUGHNESS ON TRANSITION ON A FLAT PLATE. Robert A. Jones.
March 1959. 43p. diagrs., photos., tab.
(NASA MEMORANDUM 2-9-59L)

An optical method was used to study the effect of turbulence level and sandpaper-type roughness on transition for a flat plate at a Mach number of 3 with no heat transfer. A range of roughness Reynolds number and a range of roughness height to boundary-layer displacement thickness which moved transition less than 10 percent were found and were functions of turbulence level.

Copies obtainable from NASA, Washington

1. Flow, Supersonic (1.1.2.3)
2. Flow, Laminar (1.1.3.1)
3. Flow, Turbulent (1.1.3.2)
4. Bodies - Surface Conditions (1.3.2.4)

I. Jones, Robert A.
II. NASA MEMO 2-9-59L

NASA

NASA MEMO 2-9-59L
National Aeronautics and Space Administration.
AN EXPERIMENTAL STUDY AT A MACH NUMBER OF 3 OF THE EFFECT OF TURBULENCE LEVEL AND SANDPAPER-TYPE ROUGHNESS ON TRANSITION ON A FLAT PLATE. Robert A. Jones.
March 1959. 43p. diagrs., photos., tab.
(NASA MEMORANDUM 2-9-59L)

An optical method was used to study the effect of turbulence level and sandpaper-type roughness on transition for a flat plate at a Mach number of 3 with no heat transfer. A range of roughness Reynolds number and a range of roughness height to boundary-layer displacement thickness which moved transition less than 10 percent were found and were functions of turbulence level.

Copies obtainable from NASA, Washington

1. Flow, Supersonic (1.1.2.3)
2. Flow, Laminar (1.1.3.1)
3. Flow, Turbulent (1.1.3.2)
4. Bodies - Surface Conditions (1.3.2.4)

I. Jones, Robert A.
II. NASA MEMO 2-9-59L

NASA

NASA MEMO 2-9-59L
National Aeronautics and Space Administration.
AN EXPERIMENTAL STUDY AT A MACH NUMBER OF 3 OF THE EFFECT OF TURBULENCE LEVEL AND SANDPAPER-TYPE ROUGHNESS ON TRANSITION ON A FLAT PLATE. Robert A. Jones.
March 1959. 43p. diagrs., photos., tab.
(NASA MEMORANDUM 2-9-59L)

An optical method was used to study the effect of turbulence level and sandpaper-type roughness on transition for a flat plate at a Mach number of 3 with no heat transfer. A range of roughness Reynolds number and a range of roughness height to boundary-layer displacement thickness which moved transition less than 10 percent were found and were functions of turbulence level.

Copies obtainable from NASA, Washington

1. Flow, Supersonic (1.1.2.3)
2. Flow, Laminar (1.1.3.1)
3. Flow, Turbulent (1.1.3.2)
4. Bodies - Surface Conditions (1.3.2.4)

I. Jones, Robert A.
II. NASA MEMO 2-9-59L

NASA

NASA MEMO 2-9-59L
National Aeronautics and Space Administration.
AN EXPERIMENTAL STUDY AT A MACH NUMBER OF 3 OF THE EFFECT OF TURBULENCE LEVEL AND SANDPAPER-TYPE ROUGHNESS ON TRANSITION ON A FLAT PLATE. Robert A. Jones.
March 1959. 43p. diagrs., photos., tab.
(NASA MEMORANDUM 2-9-59L)

An optical method was used to study the effect of turbulence level and sandpaper-type roughness on transition for a flat plate at a Mach number of 3 with no heat transfer. A range of roughness Reynolds number and a range of roughness height to boundary-layer displacement thickness which moved transition less than 10 percent were found and were functions of turbulence level.

Copies obtainable from NASA, Washington

1. Flow, Supersonic (1.1.2.3)
2. Flow, Laminar (1.1.3.1)
3. Flow, Turbulent (1.1.3.2)
4. Bodies - Surface Conditions (1.3.2.4)

I. Jones, Robert A.
II. NASA MEMO 2-9-59L

NASA